Technische Universität München
TUM School of Life Sciences

The key role of stomatal conductance in controlling the grassland vegetation response to a changing environment

Evidence from long-term reconstructive studies and controlled experiments

Juan Carlos Baca Cabrera

Vollständiger Abdruck der von der TUM School of Life Sciences der Technischen Universität München zur Erlangung des akademischen Grades eines

Doktors der Naturwissenschaften

genehmigten Dissertation.

Vorsitzender: Prof. Dr. Johannes Kollmann
Prüfer der Dissertation: 1. Prof. Dr. Johannes Schnyder
2. Prof. Dr. Erwin Grill
3. Prof. Dr. Gilles Lemaire

Die Dissertation wurde am 27.09.2021 bei der Technischen Universität München eingereicht und durch die TUM School of Life Sciences am 09.03.2022 angenommen.

Summary

Aims. The anthropogenic increase of atmospheric CO_2 concentration (c_a) and associated climate change are altering the biogeochemical cycles of terrestrial ecosystems. Stomata, the small pores on plant leaves which control the CO_2 and water vapor fluxes of vegetation, play a pivotal role in these cycles: they optimize the balance between carbon gain (photosynthesis) and water loss (transpiration) through adjustments of stomatal conductance (g_s) in response to environmental conditions, particularly c_a and vapor pressure deficit (VPD). Large g_s changes are expected as a consequence of climate change in grassland ecosystems, which could affect other key physiological parameters such as growth, transpiration or water-use efficiency (WUE). In this context, the aim of this work was to improve the understanding of the g_s-response of C_3 grassland vegetation to parameters of global change at two different scales: (1) the historical changes (last 100 years) in canopy stomatal conductance of grassland ecosystems and their link with WUE changes, yield trends, nitrogen acquisition and plant functional group composition; and (2) the g_s-response of perennial ryegrass (*Lolium perenne*) to CO_2 and VPD and its effect on leaf hydraulic status and leaf growth in a controlled environment. Additionally, (3) I explored some basic physiological unknowns in the process-chain that determines $\delta^{18}O$ of plant cellulose, a widely used proxy for reconstructions of g_s changes.

Materials and Methods. The investigation included observations from a long-term field experiment (Park Grass Experiment at Rothamsted, U.K.), a controlled mesocosm experiment and process-based modelling of a grassland ecosystem at Grünschwaige, near Freising, Germany. At Park Grass, the oldest continuous grassland experiment of the world, I obtained plant samples from plots receiving a wide range of different fertilizer rates and combinations for two 15 years-long periods at the beginning and the end of the last 100 years and measured the carbon isotope composition of bulk biomass ($\delta^{13}C$, a proxy for intrinsic WUE, the ratio of net photosynthesis and stomatal conductance), $\delta^{18}O$ of cellulose ($\delta^{18}O_{cellulose}$, a proxy for stomatal conductance) and C and N elemental concentration. The measurements were combined with meteorological, yield and botanical composition data to estimate the long-term response of different plant functional groups (grass-rich or dicot-rich communities) to the anthropogenic c_a-increase. In the controlled experiment, canopies of *L. perenne* were grown in a 16 h/8 h day/night regime with a 3 x 2 factorial design: three c_a levels ('half-ambient', 'ambient' and 'double-ambient') and low or high daytime VPD. When stands had formed a closed canopy, with a leaf area index >5, measurements of g_s, leaf- and canopy-scale transpiration, leaf elongation, water- and osmotic potential and turgor were performed during the day and the night, and plant

material was sampled for morphometric and oxygen isotope composition ($\delta^{18}O$) analyses. Finally, the isotope-enabled soil–vegetation–atmosphere transfer model MuSICA was parametrized for the Grünschwaige grassland and applied to simulate CO_2, energy and water fluxes, and $\delta^{18}O$ of source and leaf water and $\delta^{18}O$ of cellulose ($\delta^{18}O_{cellulose}$) in a multi-seasonal study (2006-2012).

Results and Discussion. The Park Grass experiment showed a significant increase of $\delta^{18}O_{cellulose}$ during the last century, which indicated a systematic negative g_s-response to the changing climate. Remarkably, the g_s-response was much greater in grass-rich than in dicot-rich communities. Reductions of stomatal conductance were linked with reductions of yield trends, nitrogen acquisition, and nitrogen nutrition index and limited the CO_2-response of grasslands during the last century (indicating CO_2-saturation), despite a systematic increase in WUE during this period. In the *L. perenne* mesocosm experiment, I also observed strong effects of CO_2 and VPD on g_s and transpiration that affected the water potential of leaves. Interestingly, however, these treatments had no effect on daily leaf elongation or morphometric parameters of leaves, as they altered the difference between leaf elongation rate during the day (LER_{day}) and the night (LER_{night}) in a compensating fashion. This was associated with a significant effect of leaf transpiration on leaf water potential, which resulted in a significant decrease in turgor and LER_{day} with increasing leaf transpiration. The daytime hydraulic limitation was compensated by nighttime stored-growth controls on LER. The enhancement of LER_{night} over LER_{day} was proportional to the turgor-change between day and night, indicating complex feedbacks between g_s, transpiration, leaf hydraulics and leaf elongation under changing c_a and VPD conditions. Finally, I discuss uncertainties regarding $^{18}O_{cellulose}$ as a proxy for g_s in paleo-climatological studies, based on the $\delta^{18}O_{cellulose}$ measurements at Park Grass, the $\delta^{18}O$ analysis of leaf water, leaf sucrose and leaf cellulose in the *L. perenne* mesocosm experiment and process-based modelling of $\delta^{18}O_{cellulose}$ of the Grünschwaige grassland.

Conclusion. This work indicated a strong sensitivity of g_s to changes in CO_2 and VPD in grassland vegetation. g_s-changes altered plant transpiration and this also indirectly or directly affected yield and related physiological processes such as leaf growth, nitrogen acquisition and WUE. The results contribute to a better understanding of the stomatal conductance of grasses in a changing environment and may help to improve simulations of the biogeochemical cycles of grassland ecosystems. Finally, my results highlight the importance of reconstructive studies and also reveal that key predictions for future events (e.g. the CO_2-saturation of C_3 grasses) have already materialized in the last century.

Zusammenfassung

Zielsetzung. Der anthropogene Anstieg der atmosphärischen CO_2-Konzentration (c_a) und der damit verbundene Klimawandel verändern die biogeochemischen Kreisläufe terrestrischer Ökosysteme. Spaltöffnungen, die kleinen Poren auf Pflanzenblättern, die die CO_2- und Wasserdampfströme der Vegetation steuern, spielen in diesen Kreisläufen eine zentrale Rolle: sie optimieren das Gleichgewicht zwischen Kohlenstoffgewinn (Photosynthese) und Wasserverlust (Transpiration) durch die Anpassung der stomatären Leitfähigkeit (g_s) als Reaktion auf die Umweltbedingungen, insbesondere c_a und das Dampfdruckdefizit (VPD). Als Folge des Klimawandels werden in Graslandökosystemen große g_s-Veränderungen erwartet, die sich auf andere wichtige physiologische Parameter wie Wachstum, Transpiration oder Wassernutzungseffizienz (WUE) auswirken können. In diesem Zusammenhang war es das Ziel dieser Arbeit, das Wissen über die g_s-Reaktion von C_3-Graslandvegetation auf Parameter des globalen Wandels auf zwei verschiedenen Ebenen zu erweitern: (1) die historischen Veränderungen (in den letzten 100 Jahren) der stomatären Leitfähigkeit von Graslandökosystemen und deren Zusammenhang mit WUE-Veränderungen, Ertragstrends, Stickstoffaufnahme und der Zusammensetzung von funktionellen Pflanzengruppen; und (2) die g_s-Reaktion vom Deutschen Weidelgras (*Lolium perenne*) auf CO_2 und VPD und deren Auswirkung auf die Blatthydraulik und das Blattwachstum in einem kontrollierten Experiment. Darüber hinaus (3) untersuchte ich grundlegende physiologische Unbekannte in der Prozesskette zur Bildung der $\delta^{18}O$ von Pflanzenzellulose, einem weit verbreiteten Proxy für die Rekonstruktion von g_s-Veränderungen.

Materialen und Methoden. Die Untersuchung umfasste Beobachtungen aus einem Langzeit-Feldexperiment (Park Grass Experiment in Rothamsted, U.K.), einem kontrollierten Mesokosmen-Experiment und einer prozessbasierten Modellierung eines Graslandökosystems auf der Grünschwaige, in der Nähe von Freising, Deutschland. In Park Grass, dem ältesten kontinuierlichen Graslandexperiment der Welt, untersuchte ich die Kohlenstoffisotopenzusammensetzung von Pflanzenbiomasse ($\delta^{13}C$, ein Proxy für intrinsische WUE, das Verhältnis zwischen Nettophotosynthese und stomatärer Leitfähigkeit), $\delta^{18}O$ von Pflanzenzellulose ($\delta^{18}O_{cellulose}$, ein Proxy für die stomatäre Leitfähigkeit) sowie die C- und N-Elementarkonzentration von Pflanzenproben aus zwei 15 Jahre langen Perioden zu Beginn und am Ende der letzten 100 Jahre. Die Proben entstammten von Parzellen, die eine breite Palette unterschiedlicher Düngermengen und Düngerkombinationen erhielten. Die Messungen wurden mit meteorologischen Daten, Ertragsdaten und Daten der botanischen Zusammensetzung der Parzellen kombiniert, um

die langfristige Reaktion verschiedener funktioneller Pflanzengruppen (grasreiche oder dikotylenreiche Gemeinschaften) auf den anthropogenen c_a-Anstieg zu untersuchen. In dem kontrollierten Versuch wurden *L. perenne* Bestände in einem 16 h/8 h Tag/Nacht Regime mit einem 3 x 2 Faktor-Design angebaut: unter drei c_a-Stufen (‚Halb-Ambient', ‚Ambient' und ‚Doppel-Ambient') und unter niedrigem oder hohem Tages-VPD. Nachdem sich dichte, geschlossene Bestände entwickelt hatten (Blattflächenindex >5), wurden tags- und nachtsüber Messungen von g_s-, Blatt- und Bestandestranspiration, Blattwachstum, Wasser- und osmotischem Potenzial und Turgor durchgeführt und Pflanzenproben für morphometrische Analysen und die Analyse der Sauerstoffisotopenzusammensetzung ($\delta^{18}O$) entnommen. Schließlich wurde das isotopengestützte Boden-Vegetations-Atmosphären-Transfermodell MuSICA für das Grünschwaige Grünland parametrisiert und zur Simulation von CO_2-, Energie- und Wasserflüssen, sowie zur Bestimmung von $\delta^{18}O$ im aufgenommenen Wasser, im Blattwasser und in der Zellulose ($\delta^{18}O_{cellulose}$), in einer mehrjährigen Studie (2006-2012) angewendet.

Ergebnisse und Diskussion. Das Park Grass Experiment zeigte einen signifikanten Anstieg der $\delta^{18}O_{cellulose}$ während des letzten Jahrhunderts, was auf eine systematische negative g_s-Reaktion auf den Klimawandel hindeutet. Bemerkenswerterweise war die g_s-Reaktion in grasreichen Gemeinschaften viel größer als in dikotylenreichen Gemeinschaften. Die Reduzierung der stomatären Leitfähigkeit war mit einer Minderung der Ertragstrends, der Stickstoffaufnahme und des Stickstoffernährungsstatus verbunden und begrenzte die CO_2-Reaktion von Grasland im letzten Jahrhundert (was auf eine CO_2-Sättigung hindeutet), trotz eines systematischen Anstiegs der WUE in diesem Zeitraum. Im *L. perenne* Mesokosmen-Experiment beobachtete ich auch starke Effekte von CO_2 und VPD auf g_s und Transpiration, welche sich auf das Wasserpotenzial der Blätter auswirkte. Interessanterweise hatten die Behandlungen jedoch keine Auswirkung auf das tägliche Blattwachstum oder auf morphometrische Blattparameter, da sie die Differenz zwischen der Blattwachstumsrate während des Tages (LER_{day}) und der Nacht (LER_{night}) auf kompensierende Weise regulierten. Dies stand im Zusammenhang mit einer signifikanten Auswirkung der Blatttranspiration auf das Wasserpotenzial der Blätter, was zu einer signifikanten Abnahme des Turgors und von LER_{day} bei zunehmender Blatttranspiration führte. Die hydraulische Limitierung während des Tages wurde durch kompensierende Wachstumseffekte (‚stored-growth') in der Nacht ausgeglichen. Dabei war die Zunahme von LER_{night} gegenüber LER_{day} proportional zur Turgorveränderung zwischen Tag und Nacht, was auf komplexe Rückkopplungen zwischen g_s, Transpiration, Blatthydraulik und Blattwachstum unter wechselnden c_a- und VPD-Bedingungen hinweist. Abschließend diskutiere ich Unsicherheiten in Bezug auf $^{18}O_{cellulose}$ als Proxy für g_s in

paläoklimatologischen Studien, basierend auf den $\delta^{18}O_{cellulose}$-Messungen bei Park Grass, der $\delta^{18}O$-Analyse von Blattwasser, Blattsaccharose und Blattzellulose im *L. perenne* Mesokosmen-Experiment und der prozessbasierten Modellierung von $\delta^{18}O_{cellulose}$ des Grünschwaige Grünlands.

Schlussfolgerungen. Die vorliegende Arbeit zeigte eine starke Empfindlichkeit von g_s gegenüber Veränderungen von CO_2 und VPD in Graslandvegetation. g_s-Veränderungen beeinflussten die Pflanzentranspiration, und diese wirkte sich direkt oder indirekt auf den Ertrag und damit verknüpfte physiologische Prozesse wie Blattwachstum, Stickstoffaufnahme und WUE aus. Die Ergebnisse tragen zu einem besseren Verständnis der stomatären Leitfähigkeit von Gräsern in einer sich verändernden Umwelt bei und könnten dazu beisteuern, Simulationen der biogeochemischen Kreisläufe von Graslandökosystemen zu verbessern. Schließlich unterstreichen meine Ergebnisse die Bedeutung rekonstruktiver Studien. Sie zeigen, dass wichtige Vorhersagen für zukünftige Ereignisse (z.B. die CO_2-Sättigung von C_3-Gräsern) bereits im letzten Jahrhundert eingetreten sind.

Table of contents

List of Figures

List of Tables

1. Introduction

1.1 Grassland ecosystem responses under rising CO_2

Since the start of the industrial revolution, anthropogenic greenhouse gas emissions have caused a great increase in the CO_2 concentration in the atmosphere (c_a) from around 280 ppm to around 410 ppm today. This human-caused c_a increase and associated climate change are fundamentally altering the carbon (C), water and nutrient cycles of terrestrial ecosystems at a global scale (Körner, 2006; Feng *et al.*, 2015; Craine *et al.*, 2018; Gentine *et al.*, 2019; Du *et al.*, 2020). Out of the multiple observed effects and feedbacks (see e.g. Reich *et al.*, 2006; Field *et al.*, 2007; Arneth *et al.*, 2010; Bernacchi & VanLoocke, 2015 for reviews on this topic), one feature that has received central attention is the CO_2 fertilization effect (CFE): the Rubisco carboxylation reaction of C_3 plants is not saturated at current c_a, therefore a general increase in photosynthesis is expected under rising c_a (Bowes, 1993; Drake *et al.*, 1997). Also, high c_a suppresses photorespiration, a process that has been considered a wasteful side reaction of Rubisco and accounting for c. 25% of net photosynthesis in C_3 leaves (Dusenge *et al.*, 2019). In fact, a 30% global increase in gross primary production during the 20th century has been reported (Campbell *et al.*, 2017), which may have led to a slowdown in the rates of CO_2-accumulation in the atmosphere and of climate change (Keenan & Williams, 2018). However, the global CFE has declined constantly during the last decades across terrestrial ecosystems (Wang *et al.*, 2020), rising questions about its future trends and introducing further uncertainty to climate projections (Friedlingstein *et al.*, 2014).

Parallel to these global studies of past changes, free-air CO_2 enrichment (FACE) experiments (Ainsworth & Long, 2005) have been performed during the last 30 years to gain a deeper understanding about the future c_a response and underlying mechanisms in natural and managed ecosystems. In general, a positive CFE was confirmed in FACE experiments, but the magnitude of the response varied enormously, ranging from no response to >50% enhancement in aboveground biomass production (Nowak *et al.*, 2004; Ainsworth & Long, 2005), and differing significantly among plant functional groups (Ainsworth & Long, 2005, see also (Fig. 1.1a, b) and ecosystem types (Song *et al.*, 2019; Terrer *et al.*, 2019), with C_3 grasses and grassland ecosystems systematically showing a lower CFE and, in some experiments, even negative responses (Fig. 1.1c). Grasslands comprise around 30% of the total land area not covered by ice (Foley *et al.*, 2011; Dixon *et al.*, 2014), making them a relevant component in the global biogeochemical cycles.

Thus, understanding the mechanisms associated with the below-average response of grassland biomass production to elevated CO_2 could potentially improve our ability to predict the future development of global change.

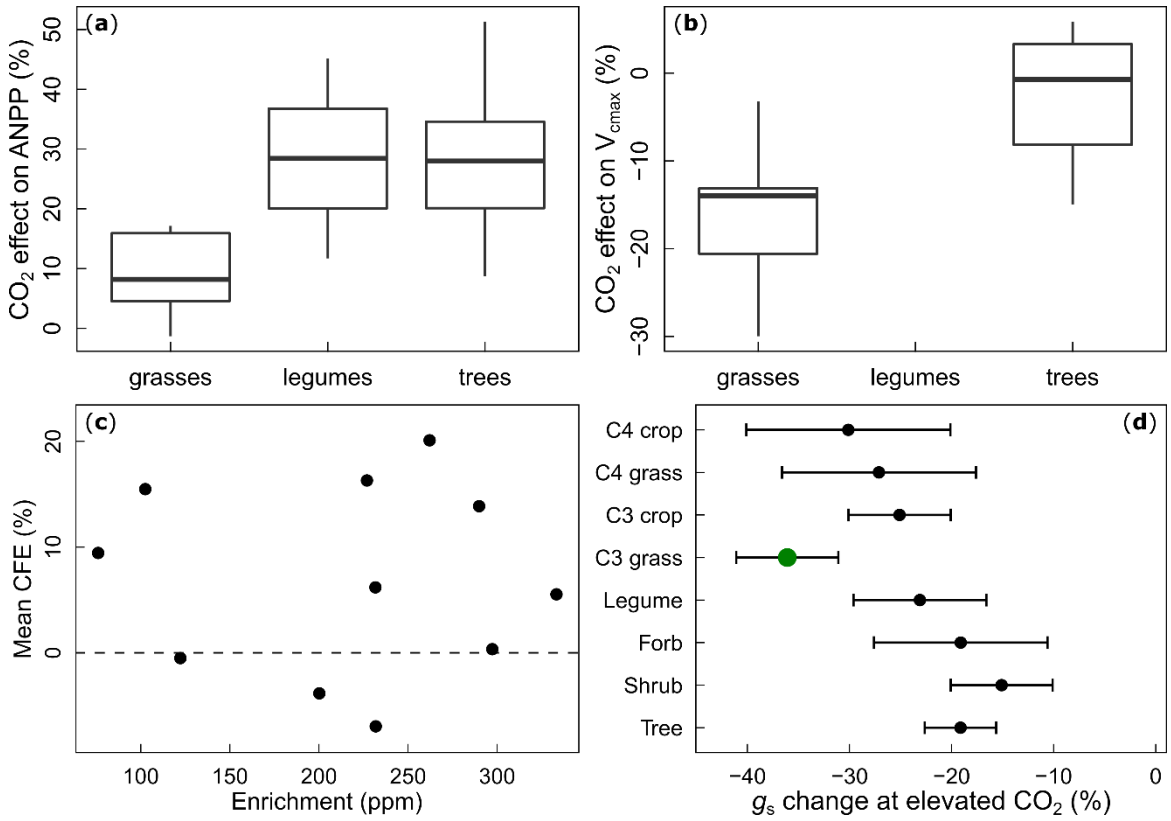

Fig. 1.1: Effect of elevated CO_2 in open-top chamber and FACE experiments. CO_2 effect on aboveground net primary production (ANPP) (**a**) and maximum rate of carboxylation (V_{cmax}) (**b**) for different functional groups in FACE experiments (adapted from Terrer *et al.*, 2018); mean CO_2 fertilization effect (CFE) of temperate C_3 grasslands under varying enrichment levels in open-top chamber and FACE experiments (**c**) (adapted from Hovenden *et al.*, 2019); and mean stomatal conductance (g_s) change (±95% CI) of different plant functional groups under elevated CO_2 in FACE experiments (**d**) (adapted from Ainsworth & Rogers, 2007).

That limitations in the CO_2 fertilization of C_3 grasslands are likely to occur and may have already happened in the past is illustrated by an investigation at Park Grass, which found no effect of increasing c_a on herbage yield trends (a proxy for photosynthesis trends, see Baca Cabrera *et al.*, 2021a) between 1891–1992 (Jenkinson *et al.*, 1994), although intrinsic water-use efficiency (the ratio between photosynthesis and stomatal conductance) has increased in the same period (Köhler *et al.*, 2010). Constraints in the CO_2 response of grasslands have been associated with increasing nitrogen and phosphorus limitation (Terrer *et al.*, 2016; Terrer *et al.*, 2019), changing seasonal distribution of precipitation (Obermeier *et al.*, 2018; Hovenden *et al.*, 2019), joint water and nitrogen limitation (Reich *et al.*, 2014) or changes in the carbon allocation strategies (Song *et al.*, 2019). But, there

is still great uncertainty about the processes underlying the CFE and its feedbacks with other biogeochemical cycles (e.g. water and nitrogen), indicating the need to integrate real world observations of climate change effects on grassland ecosystems with experimental and modelling approaches that improve the mechanistic understanding of these processes. In that context, this thesis combines observational, experimental and modelling approaches to study the effects of parameters of global change on grassland vegetation at different scales (Fig. 1.2), with a main focus on the central player governing the links between carbon, water and nutrient cycles in grassland vegetation: stomatal conductance.

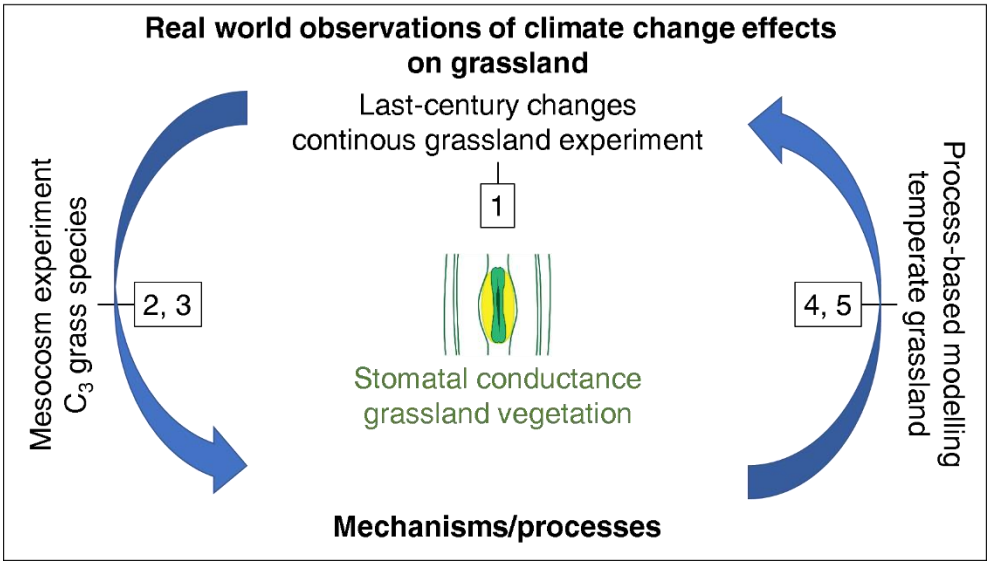

Fig. 1.2: Conceptual framework for the study of effects of parameters of global change on grassland ecosystems. Empirical evidence about long-term changes (100 years) of grassland ecosystems is obtained from isotopic and elemental analyses of herbage samples from the Park Grass Experiment (publication "1", Baca Cabrera *et al*., 2021a). This observational approach is complemented by mechanistic studies including: (i) a controlled mesocosm experiment with perennial ryegrass, in which the effects of CO_2 and vapor pressure on stomatal conductance, leaf growth processes and the oxygen isotopic composition ($\delta^{18}O$) of leaf cellulose, a proxy for stomatal conductance, are explored (publications "2" and "3", Baca Cabrera *et al.*, 2020; Baca Cabrera *et al.*, 2021b); and (ii) process-based modelling of CO_2, energy and water fluxes and $\delta^{18}O$ of different plant compartments in a temperate grassland and their relationship with meteorology and morpho-physiological traits (publications "4" and "5", Hirl *et al*., 2019; Hirl *et al*., 2021). The stomatal conductance response is a central element in all five publications, generating a main link among them (see Sections 1.4 and 2 for details on study aims and methods).

1.2 Stomata: key players in the control of water vapor and CO_2 fluxes

At local scales, the biogeochemical cycles of terrestrial ecosystem are linked by processes occurring at vegetation level, specifically at the surfaces of leaves (Hetherington & Woodward, 2003; Berry *et al.*, 2010; Medlyn *et al.*, 2011; Franks *et al.*, 2013) and roots

(McGrath & Lobell, 2013; Oyewole *et al.*, 2014; Feng *et al.*, 2015). Stomata, the small pores in the leaf epidermis, optimize the balance between CO_2 uptake by photosynthesis and water loss by transpiration through adjustments in their conductance (stomatal conductance, g_s) in response to changes in environmental conditions (Hetherington & Woodward, 2003; Medlyn *et al.*, 2011), principally c_a (Ainsworth & Rogers, 2007; Leakey *et al.*, 2009; Franks *et al.*, 2013) and vapor pressure deficit (VPD) (Katul *et al.*, 2009; Buckley, 2017; Grossiord *et al.*, 2020), and internal cues such as photosynthetic activity, a factor that strongly correlates with leaf nitrogen status (Kattge *et al.*, 2009; Smith & Keenan, 2020). Simultaneously, stomatal conductance may indirectly affect the N uptake of vegetation: when transpiration changes, the advective flux of soil water to roots changes in parallel, thus altering the mass flow dependent N uptake (McGrath & Lobell, 2013; Oyewole *et al.*, 2014). This link between stomatal conductance, photosynthesis, transpiration and N uptake (Fig. 1.3a) is a key element for understanding and predicting the acclimation of vegetation under climate change (Smith & Keenan, 2020).

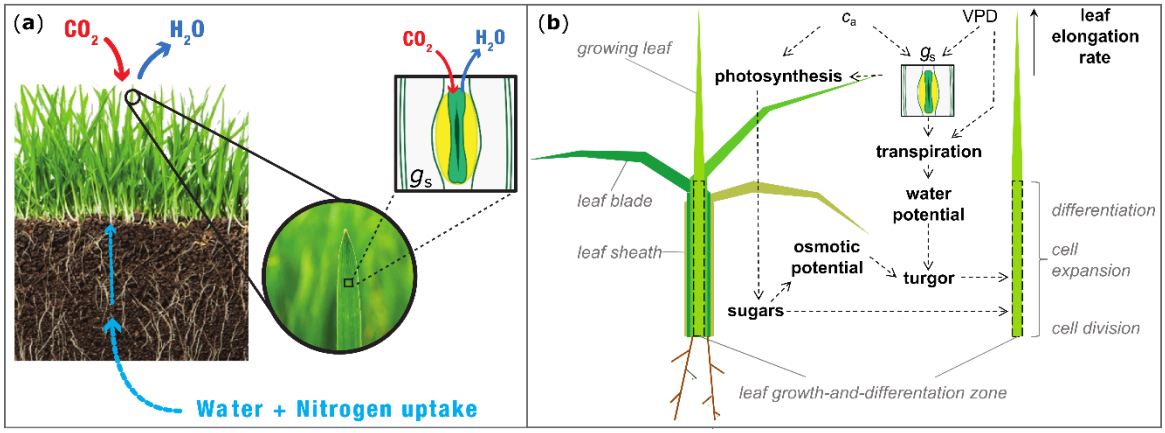

Fig. 1.3: Stomatal control of water vapor and CO_2 fluxes. Stomata actively regulate the CO_2 and H_2O exchange between vegetation and the atmosphere by adjusting their conductance (g_s) in response to changing environmental conditions, particularly atmospheric CO_2 (c_a) and vapor pressure deficit (VPD). That regulation influences key physiological processes: (**a**) the bulk flow-dependent nutrient uptake of a grassland canopy is indirectly governed by g_s, by means of canopy transpiration regulation; (**b**) (adapted from Baca Cabrera *et al.*, 2020) g_s affects leaf elongation rate of a vegetative grass leaf by influencing photosynthesis (which affects the assimilate supply for cell growth processes and the contribution of sugars to osmotic potential) and transpiration (which affects leaf hydraulics). Notice the typical "dumb-bell" shape of grass stomata with guard cells (green), and specialized subsidiary cells (yellow) surrounding the stomatal pore.

As c_a is expected to rise to more than 800 ppm at the end of the century (Friedlingstein *et al.*, 2014) and a continuous rise in VPD has also been predicted (Grossiord *et al.*, 2020), a large decrease in stomatal conductance at global scale is likely to occur. Results from FACE experiments under various environmental conditions and with

distinct plant functional groups reveal a systematic, strong decrease of stomatal conductance in C_3 vegetation at elevated CO_2 (Ainsworth & Rogers, 2007), leading to an analogous decrease in transpiration (Leakey *et al.*, 2009). Also, a negative relationship between VPD and stomatal conductance has been well documented across vascular plants (McAdam & Brodribb, 2015; Grossiord *et al.*, 2020). The decrease in stomatal conductance and transpiration could fundamentally alter the balance between carbon, nitrogen and water status of terrestrial vegetation: as transpiration decreases, mass-flow dependent nitrogen uptake is also expected to decrease, potentially leading to nitrogen limitation and a reduction of the CFE potential (McGrath & Lobell, 2013). In fact, limitations in nitrogen acquisition have been reported in elevated CO_2 studies in the field, associated with a reduction in transpiration (Feng *et al.*, 2015), and data from field experiments and herbaria collections indicate a general increase in foliar C : N ratios under rising c_a (Sardans & Peñuelas, 2012). Additionally, photosynthesis (A) and transpiration (E) are intimately linked via the stomata. Both fluxes are the products of stomatal conductance (to CO_2 or H_2O) and the concentration gradients of the respective gases:

$$A = g_{s\,CO_2}\,(c_a - c_i); \quad E = g_{s\,H_2O}\,(w_i - w_a) \tag{1.1}$$

where c_a and w_a are the CO_2 and water vapor mole fractions in the atmosphere, and c_i and w_i that in the intercellular air spaces. Thus, it becomes evident that at a specific gradient between c_i and c_a any downregulation of stomatal conductance will ultimately reduce photosynthesis.

The negative stomatal response to c_a and VPD is especially pronounced in C_3 grasses. Thus, C_3 grasses showed the largest stomatal conductance decrease under elevated CO_2 compared to other plant functional groups in FACE experiments (Fig. 1.1d) and their response to VPD has also been observed to be the highest and fastest across a spectrum of vascular plants (Franks & Farquhar, 2007). This phenomenon is associated with the unique architecture of grass stomata: the stomatal pores are surrounded by elongated “dumb-bell”-shaped guard cells (unlike the more common kidney-shaped guard cells of most of the other vascular plants) which are flanked by specialized subsidiary cells (Nunes *et al.*, 2020; see also Fig. 1.3) that allow the optimization of pore aperture and a faster and more efficient response to environmental changes compared to other stomata types (Franks & Farquhar, 2007). The stronger stomatal conductance response of C_3 grasses compared to other functional groups could partially explain why C_3 grasslands showed a below-average CFE in FACE experiments, especially in some temperate humid regions (Lüscher *et al.*, 2004; Körner, 2006).

The expected large decrease in stomatal conductance of C_3 grasses under rising c_a and VPD could also indirectly impact the C, N and water balance of vegetation via changes in growth processes at the leaf level. Leaf growth of grasses is highly sensitive to plant water status and leaf hydraulics (Pantin *et al.*, 2012; Caldeira *et al.*, 2014; Tardieu *et al.*, 2015), which are both indirectly controlled by stomatal conductance through changes in transpiration. At the same time, leaf growth depends on a sufficient nutrient availability and an adequate supply of assimilates from the leaves to the heterotrophic leaf growth-and-differentiation zone (LGDZ, Fig. 1.3b), which is the place where cell production, expansion and differentiation are occurring. As photosynthesis and transpiration respond to changes in c_a, VPD and stomatal conductance, fundamental effects on leaf growth might be expected (Fig. 1.3b). Surprisingly, strong effects of c_a on leaf growth have not generally been observed, and the response magnitude was found to depend on various co-varying factors, including N-limitation (see e.g. Ferris *et al.*, 1996; Masle, 2000; Seneweera & Conroy, 2005). This points to the necessity of more detailled research on the mechanisms linking stomatal conductance, photosynthesis, transpiration, leaf hydraulics and leaf growth in grasses, particularly under conditions of low N-availability, a situation commonly observed in the field, including in grassland ecosystems (LeBauer & Treseder, 2008).

An additional challenge in the study of the stomatal conductance response of grasses to environmental changes and its implications for biogeochemical cycles is the perspective of scale. Stomatal conductance can be measured at leaf, canopy or ecosystem scales, using leaf gas exchange, stable isotopes or eddy-flux techniques. However, values obtained at one scale cannot always be directly extrapolated to another by a simple exercise of up-and down scaling. This was clearly shown recently, as g_1 (a model parameter describing the sensitivity of stomatal conductance to c_a, photosynthesis and VPD, Medlyn *et al*., 2011) of various functional groups differed greatly if it was estimated from eddy-flux or leaf gas exchange global datasets (Medlyn *et al.*, 2017). Additionally, expanding the temporal scale of studies could considerably improve our understanding of long-term effects in grassland ecosystems. Most of the gained knowledge regarding this theme comes from data obtained from FACE experiments (Ainsworth & Rogers, 2007) or eddy-flux measurements (Friend *et al.*, 2007), both of which are no older than 30 years, so reconstructive studies are needed to capture responses at longer time scales (e.g. a century).

1.3 Use of oxygen and carbon isotopes for the study of stomatal conductance changes

The use of stable isotopes has established itself as a valuable tool in plant physiology research during the last decades. The carbon and oxygen isotopic composition ($\delta^{13}C$ and $\delta^{18}O$) of plant material can provide insights about the physiological processes (e.g. stomatal conductance, mesophyll conductance, water-use efficiency, etc.) and responses of vegetation under a changing environment, across a broad range of spatial (from the leaf to the ecosystem) and temporal scales (from immediate responses to centuries) (Ehleringer *et al.*, 1993; Dawson *et al.*, 2002). The relationship between ^{13}C-discrimination ($\Delta^{13}C$) and intrinsic water-use efficiency (WUE_i) is – for the most part – well understood and has been widely tested across scales (Seibt *et al.*, 2008). WUE_i, the physiological, i.e. non-climatic component of water-use efficiency (WUE), represents the ratio between photosynthesis and stomatal conductance:

$$\mathrm{WUE}_i = \mathrm{WUE}(w_i - w_a) = \frac{A}{g_{s\,H_2O}} = \frac{g_{s\,CO_2}(c_a - c_i)}{g_{s\,H_2O}} = \frac{c_a - c_i}{1.6} = \frac{c_a\left(1 - \frac{c_i}{c_a}\right)}{1.6} \quad (1.2)$$

with 1.6 the ratio of the diffusivities of water vapor and CO_2 (Farquhar & Richards, 1984; Cernusak *et al.*, 2013). According to the simplified version of the Farquhar *et al.* (1982) model, c_i/c_a is linearly related to $\Delta^{13}C$ (see details in Materials and Methods), so records of $\delta^{13}C$ of plant material can be used to determine long-term (assimilation-weighted) changes in intrinsic water-use efficiency. For instance, $\Delta^{13}C$ studies have shown large increases in WUE_i (≈ 20-30%) in alpine (Barbosa *et al.*, 2010; Rosbakh *et al.*, 2021) and temperate grasslands (Köhler *et al.*, 2010) during the last century, but it could not be determined whether these long-term changes were governed by an increase in photosynthesis, a decrease in stomatal conductance or a combination of both. The use of the so-called dual carbon/oxygen isotope approach (Scheidegger *et al.*, 2000) has been suggested as a method to disentangle the effect of photosynthesis and stomatal conductance on WUE_i. This is based on theoretical considerations (Farquhar *et al.*, 1998) and observations (Barbour *et al.*, 2000; Sullivan & Welker, 2007; Grams *et al.*, 2007; Moreno-Gutiérrez *et al.*, 2012) of a negative relationship between stomatal conductance and $\delta^{18}O$ of plant cellulose ($\delta^{18}O_{cellulose}$).

The negative relationship between stomatal conductance and $\delta^{18}O_{cellulose}$ (or of its enrichment above source water, $\Delta^{18}O_{cellulose}$) is complex and not fully understood (Fig. 1.4a). The connection is primarily determined by three factors: (1) all oxygen in plant cellulose ultimately originates from water (DeNiro & Epstein, 1979; Liu *et al.*, 2016); (2) a

large proportion of that water is evaporatively enriched leaf water that imprints its ^{18}O signal onto sucrose – the most ubiquitous primary photosynthetic product and translocated sugar – and is used for cellulose synthesis in growing sink tissues; and (3) according to theory, evaporative ^{18}O-enrichment of leaf water ($\Delta^{18}O_{LW}$) decreases with increasing stomatal conductance (Barbour, 2007). $\Delta^{18}O_{LW}$ has been generally assumed to be equal to the ^{18}O-enrichment of water at the site of photosynthesis, which has been supported primarily by investigations of leaf water and phloem sap organic matter in two dicot species (Cernusak *et al.*, 2003; Cernusak *et al.*, 2005). This assumption is also practical, as measurements of $\Delta^{18}O_{LW}$ are simple in comparison to estimations of ^{18}O-enrichment at the site of sucrose synthesis ($\Delta^{18}O_{SucSynW}$), but could lead to errors in the interpretation of ^{18}O signals in grasses (Lehmann *et al.*, 2017; Hirl *et al.*, 2021). Current mechanistic understanding of the relationship between $\Delta^{18}O_{Cellulose}$ and $\Delta^{18}O_{SucSynW}$ can be summarized (Barbour & Farquhar, 2000; Baca Cabrera *et al.*, 2021b) as:

$$\Delta^{18}O_{Cellulose} = \Delta^{18}O_{SucSynW}\,(1 - p_{ex}p_x) + \varepsilon_{bio}, \qquad (1.3)$$

with p_x the proportion of unenriched source water at the site of cellulose synthesis, p_{ex} the proportion of oxygen atoms in cellulose that exchanges with medium water during cellulose formation and ε_{bio} the temperature dependent biochemical fractionation between carbonyl oxygen and water (Sternberg & Ellsworth, 2011). The term $p_{ex}p_x$ represents the proportion of the original ^{18}O signal that is lost during cellulose synthesis and is often set as a constant at ~0.4 (Barbour, 2007). While p_x is close to 1 in grasses (Liu *et al.*, 2017), p_{ex} was found to vary under changing environmental conditions when $\Delta^{18}O_{SucSynW}$ was set equal with $\Delta^{18}O_{LW}$ (Song *et al.*, 2014; Hirl *et al.*, 2021). Unfortunately, knowledge of $\Delta^{18}O_{SucSynW}$ and its relationship with $\Delta^{18}O_{LW}$ is scarce (Lehmann *et al.*, 2017), so that the true relationship between $\Delta^{18}O_{SucSynW}$ and $\Delta^{18}O_{Cellulose}$ is largely unknown. For that, and potentially other reasons, the mechanistic relationship between $\Delta^{18}O_{cellulose}$ or $\delta^{18}O_{cellulose}$ and stomatal conductance is still unknown (Roden & Siegwolf, 2012).

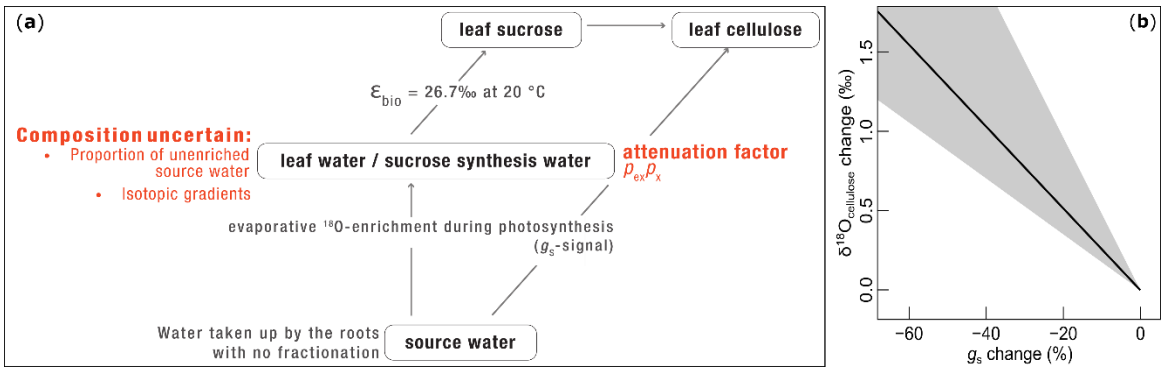

Fig. 1.4: Relationship between stomatal conductance and δ^{18}O of leaf cellulose (δ$^{18}O_{cellulose}$). (**a**): conceptual diagram of the process-chain determining δ^{18}O of leaf cellulose (δ$^{18}O_{cellulose}$). The ^{18}O-enrichment of leaf water is expected to decrease with increasing g_s (Barbour, 2007), but the ^{18}O composition of the leaf water used for sucrose synthesis is still uncertain, due to large variability in the fraction of unenriched sourced water in leaf water (Cernusak *et al.*, 2016), strong and variable longitudinal isotopic gradients, particulary in grasses (Helliker & Ehleringer, 2000; Gan *et al.*, 2003), and ignorance of the (corresponding) spatial distribution of photosynthesis and associated sucrose synthesis along leaves. Also, the attenuation factor $p_{ex}p_x$ (the fraction of the original ^{18}O-enrichment signal in sucrose that is subsequently lost during cellulose synthesis) is not well constrained. (**b**): sensitivity of δ$^{18}O_{cellulose}$ increase (in per mil) to g_s changes (in %-g_s change), based on empirical observations in different plant species in a range of environmental conditions (adapted from Baca Cabrera *et al.*, 2021a).

Regardless of the aforementioned challenges, δ$^{18}O_{cellulose}$ is still considered a robust (at least semi-quantitative) predictor of stomatal conductance changes, particularly for the study of temporal changes and comparisons among species or functional groups in the same environment (see e.g. Barnard *et al.*, 2012; Giuggiola *et al.*, 2016; Guerrieri *et al.*, 2019). Additionally, the average sensitivity of δ$^{18}O_{cellulose}$ to changes in stomatal conductance can be estimated from studies that have analyzed this relationship directly (Fig. 1.4b), allowing more accurate interpretations of g_s/δ$^{18}O_{cellulose}$ long-term changes. Finally, process-based modelling and controlled experiments may be applied to improve the mechanistic understanding of the ^{18}O signal transfer from leaf water to leaf cellulose under changing c_a and VPD conditions. In that, the uncertainty associated with the use of δ$^{18}O_{cellulose}$ as a surrogate for stomatal conductance could be reduced.

1.4 Aims and outline of the thesis

The general aim of this work was to investigate the response of stomatal conductance of C_3 grassland vegetation to parameters of global change, combining real world observations with experimental and modelling approaches. In that, this thesis includes: (1) observations of historical changes (last 100 years) at Park Grass; (2) a controlled mesocosm experiment in which the physiological responses of perennial ryegrass (*Lolium*

perenne, my model C_3 grass species) to c_a and vapor pressure deficit were investigated; and (3) process-based modelling of a C_3 temperate grassland ecosystem. The challenge here was to integrate such contrasting temporal and spatial scales and methodological approaches in the study of C_3 grassland vegetation responses to global change drivers.

In a first step, I reconstructed the long-term changes in stomatal conductance that occurred during the last century at Park Grass, and its implications in terms of CFE limitations of grassland ecosystems under N-limited conditions (publication "1"). For this, elemental and isotopic analyses of archived herbage samples were performed. Using $\delta^{13}C$ and $\delta^{18}O_{cellulose}$ as proxies for intrinsic water-use efficiency (WUE_i) and stomatal conductance, respectively, I evaluated: (1) the effect of rising c_a on WUE_i, yield, stomatal conductance and N-acquisition for a wide range of grassland communities; (2) the differences in long-term responses associated with plant functional group composition (grass-rich communities vs. dicot-rich communities); and (3) the relationship between the stomatal conductance response and the long-term trends in yield, WUE_i, and nitrogen nutrition.

Secondly, I explored the effects of c_a (Last Glacial Maximum, "half-ambient"; present-day, "ambient"; and end of the century projections, "elevated") and VPD (low or high VPD) on stomatal conductance and putative mechanisms controlling leaf elongation in perennial ryegrass, under conditions of low N-availability in a mesocosm experiment (publication "2"). The specific aims were: (1) to evaluate the effect of CO_2, VPD and their interaction on stomatal conductance; (2) to determine if stomatal conductance changes affected leaf growth processes by means of hydraulic limitation; (3) to explore the effect of elevated CO_2 on leaf growth and its magnitude (is there a CFE?); and (4) to examine the diurnal oscillation of leaf growth under changing environmental conditions. Also, as part of the same experiment, I analyzed uncertainties in the process-chain determining $\delta^{18}O_{cellulose}$ in perennial ryegrass (publication "3"). In that, I determined the ^{18}O-enrichment of bulk leaf water ($\Delta^{18}O_{LW}$), leaf sucrose ($\Delta^{18}O_{Sucrose}$) and leaf cellulose ($\Delta^{18}O_{Cellulose}$) under contrasting c_a and VPD levels, and asked: (1): Do CO_2, VPD or their interactions affect the discrepancy between the ^{18}O-enrichment of bulk leaf water ($\Delta^{18}O_{LW}$) and sucrose synthesis water ($\Delta^{18}O_{SucSynW}$)? (2) Are there diurnal trends in $\delta^{18}O_{sucrose}$ and are these reflected in $\delta^{18}O_{cellulose}$? And (3) does the attenuation factor (p_{ex}/p_x) vary across c_a and VPD gradients?

Finally, I contributed to a study of CO_2, energy and water fluxes and ^{18}O-enrichment of multiple compartments of a temperate grassland ecosystem with a process-based isotope-enabled model MuSICA (publications "4" and "5"). That model included a new allocation-and-growth module, and permitted simulation of physiological processes,

including canopy stomatal conductance and its relationship with ^{18}O-enrichment of leaf cellulose in Grünschwaige temperate humid grassland with a resolution of 30 minutes over seasonal and multiannual (2006-2012) time scales. This work generated new insights into the effect of environmental parameters on the mechanistic relationship between ^{18}O-enrichment of leaf water and cellulose and their connections with canopy stomatal conductance.

Accordingly, this thesis has the following structure: Chapter 2 synthesizes the experimental design and the principal measurements performed at the Park Grass site and in the mesocosm experiment, and the statistical methods used for their evaluation. Also, it summarizes the methods applied for the analysis and interpretation of $\delta^{18}O$ of plant compartments in the mesocosm experiment and the modelling study. Chapter 3 presents the abstracts of the publications that are included in this dissertation. And, Chapter 4 discusses the most important results of the investigation, which include: evidence of a consistent decrease of stomatal conductance of grassland vegetation under rising c_a and VPD across temporal and spatial scales (Section 4.1), the limitations imposed by stomatal conductance on the carbon fertilization effect and leaf growth (Section 4.2), and the confirmation of $\delta^{18}O_{cellulose}$ as a valid tool for semi-quantitative estimations of stomatal conductance changes (Section 4.3). Finally, I present the conclusions of this work and the perspectives for future investigations in Section 4.4.

2. Materials and Methods

2.1 The Park Grass Experiment

2.1.1 Experimental design and sampling

The Park Grass Experiment (Storkey *et al.*, 2015) (hereafter referred to as Park Grass), located at the Rothamsted Research Station in Hertfordshire, U.K., approx. 40 km north of London, is the oldest permanent grassland experiment in the world. Started in 1856 in a semi-natural temperate humid grassland, the experiment comprises 20 main plots with different fertilizer inputs, and most of the main plots have been further divided into subplots that receive different lime inputs. A complete description of fertilizer treatments and experimental design is available in Macdonald *et al.* (2018). Since the beginning of the experiment, herbage has been cut in mid-June (spring growth) and representative samples of dried herbage have been stored in the Rothamsted Sample Archive (Silvertown *et al.*, 2006). The original vegetation at Park Grass was classified post-hoc as a mesotrophic, dicotyledon-rich grassland (Dodd *et al.*, 1994), but the plant functional group composition has changed dramatically since the beginning of the experiment as a consequence of the fertilizer and lime treatments, resulting in very contrasting community compositions.

Here, I selected twelve treatments (13 plots) with contrasting fertilizer and lime treatments, ranging from no fertilizer application (control plots) to high inputs of nitrogen, phosphorus and potassium. Together, these treatments led to large variations in total herbage yield and plant functional group composition (grasses, forbs, legumes, Table 2.1). To investigate the long-term changes in intrinsic water-use efficiency, yield, stomatal conductance and nitrogen acquisition that have occurred during the last century, representative subsamples (2-3 g) of plant material were taken from the Rothamsted sample archive. The samples corresponded to two 15-year periods at the beginning (1917–1931, period 1) and the end (2004–2018, period 2) of the last 100 years, and were used for a series of elemental and isotopic analyses (see Section 2.1.2). The period length was chosen to ascertain robust long-term comparisons that account for the large interannual variability of the parameters of interest.

Table 2.1: Summary of the most important characteristics of the selected treatments. A more detailed version of this table including information about plot distribution, species richness and the methods used for the determination of plant functional group (PFG) composition and nutrient limitation can be found in (Baca Cabrera *et al*., 2021a). Nitrogen (N) was applied either as ammonium sulphate or sodium nitrate; phosphorus/potassium (P/K) were applied as triple superphosphate and potassium sulphate, respectively. Treatments with a grass proportion >80% were termed grass-rich, and the others were termed dicot-rich. The letter "L" (limed) and "U" (unlimed) in the treatment names indicate if chalk was applied.

Treatment	P/K input ($g\ m^{-2}\ yr^{-1}$)	N input ($g\ m^{-2}\ yr^{-1}$)	PFG composition (%-grass/%-forb/%-legume)	Herbage yield ($g\ m^{-2}$)	Nutrient limitation
CONTROL.L	0/0	0	Dicot-rich (48/40/12)	224	co-limitation
CONTROL.U	0/0	0	Dicot-rich (63/33/4)	149	co-limitation
PK.L	3.5/22.5	0	Dicot-rich (54/21/25)	501	N-limitation
N*1.L	0/0	4.8	Dicot-rich (62/36/2)	244	co-limitation
N*1PK.L	3.5/22.5	4.8	Dicot-rich (68/20/12)	496	N-limitation
N*2.PK.L	3.5/22.5	9.6	Grass-rich (80/17/3)	487	co-limitation
N1.L	0/0	4.8	Dicot-rich (66/33/1)	208	co-limitation
N1.U	0/0	4.8	Grass-rich (97/3/0)	100	co-limitation
N2PK.L	3.5/22.5	9.6	Grass-rich (90/7/3)	545	N-limitation
N2PK.U	3.5/22.5	9.6	Grass-rich (99/1/0)	355	N-limitation
N3PK.L	3.5/22.5	14.4	Grass-rich (91/9/0)	560	N-limitation
N3PK.U	3.5/22.5	14.4	Grass-rich (100/0/0)	374	co-limitation

2.1.2 Performed analyses

The long-term changes at Park Grass were investigated based on elemental and isotopic analyses of herbage samples from the Rothamsted sample archive, combined with datasets about herbage yields, plant functional composition, meteorology and atmospheric CO_2 concentration at this location. A detailed description of the methods has been presented in Baca Cabrera *et al.* (2021a). Here, I briefly summarize the performed analyses and the data obtained.

Elemental and isotope analyses

Aliquots of 0.7±0.05 mg of sampled material were weighed into tin cups and measured by isotope ratio mass spectrometry (IRMS) as in Baca Cabrera *et al.* (2021a), to obtain the

carbon isotope composition of bulk plant material ($\delta^{13}C_p$) and the C and N elemental concentration (%C and %N in dry biomass). Additionally, α-cellulose was extracted from 50 mg of dry sample material by following the protocol by Brendel *et al.* (2000) as modified by Gaudinski *et al.* (2005) and $\delta^{18}O_{cellulose}$ was measured by IRMS, using the same method as for bulk plant material.

Herbage yield, nitrogen acquisition, plant functional composition and meteorology datasets

Additional datasets corresponding to Park Grass were obtained from the electronic Rothamsted Archive (e-RA, http://www.era.rothamsted.ac.uk/). Total herbage yield data from the first cut (spring growth, expressed in g dry biomass m^{-2} yr^{-1}) was obtained for the period 1917–2018. Due to a change in the harvest method since 1960, yield data between 1917–1959 had to be corrected with a treatment-specific correction factor (see the Method section in Baca Cabrera *et al.*, 2021a for details). Nitrogen acquisition (N acquisition, g m^{-2} yr^{-1}) was calculated as yield × N concentration. The plant functional composition (%-grasses, %-forbs and %-legumes in standing dry biomass) was calculated from observations made between 1915–1976, 1991–2000 and 2010–2012. Comparisons between communities were based on the proportion of grasses: treatments with a grass proportion >80% were defined as grass-rich, and the remaining treatments as dicot-rich. Daily meteorological data (temperature, relative humidity, vapor pressure deficit and precipitation) between 1 April and 30 June were obtained for the last 100 years (1917–2018) and used to calculate yearly spring averages. Long-term climatic changes were estimated from the spring averages.

Intrinsic water-use efficiency and stomatal conductance

According to the simple Farquhar *et al.* (1982) model of ^{13}C-discrimination ($\Delta^{13}C$) in C_3 plants, $\Delta^{13}C$ is linearly related to the c_i/c_a ratio as:

$$\Delta^{13}C = a + (b - a)\frac{c_i}{c_a}, \quad (2.1)$$

where a is the ^{13}C-discrimination during diffusion of CO_2 through the stomata (4.4‰), and b the discrimination due to Rubisco carboxylation (27‰) (Farquhar *et al.*, 1989), so that the intrinsic water-use efficiency (WUE_i, the ratio between photosynthesis and stomatal conductance, see Eqn 1.2) can be calculated if c_a and $\Delta^{13}C$ are known. A new version of the Farquhar model that also accounts for effects of mesophyll conductance and photorespiration on $\Delta^{13}C$ (Ma *et al.*, 2021) was used for this purpose. $\Delta^{13}C$ was estimated from the C isotope composition of the sample ($\delta^{13}C_p$) and that of atmospheric CO_2 ($\delta^{13}C_a$), as:

$$\Delta^{13}C = \frac{\delta^{13}C_a - \delta^{13}C_p}{1 + \delta^{13}C_p}, \quad (2.2$$

with c_a and $\delta^{13}C_a$ obtained from ice core records (Friedli *et al.*, 1986) and atmospheric monitoring stations (White *et al.*, 2015; Dlugokencky *et al.*, 2019).

The c_i/c_a ratio was also used to estimate a canopy-scale, growing season-integrated, stomatal conductance (g_s, in mol m^{-2} s^{-1}). Following reasoning in Farquhar & Richards (1984):

$$g_s = A / (c_a (1 - c_i/c_a)) = Y / (c_a (1 - c_i/c_a)/(1 - \phi)(1 - r)), \quad (2.3)$$

with Y the total herbage yield, ϕ the proportion of carbon respired and r that allocated to roots and non-harvested shoot biomass. As measurements of A were unavailable, we used yield as a proxy and assumed constant ϕ (0.35) and r (0.4) values for the last 100 years. This yield-based stomatal conductance (hereafter $g_{s\ yield}$) was used as a complement for $\delta^{18}O_{cellulose}$ to evaluate long-term stomatal conductance changes at Park Grass.

2.1.3 Statistical analysis

The statistical methods used for the Park Grass study have been described in detail in Baca Cabrera *et al.* (2021a). In brief, long-term changes were defined as significant differences between period 1 (1917–1931) and 2 (2004–2018), for each parameters of interest. t-tests were run for (1) every treatment individually, (2) grouping the data into dicot-rich and grass-rich treatments and (3) combining all data together. Additional t-tests were performed to test significant differences in the long-term responses of dicot-rich vs. grass-rich communities. Additionally, the relationship between the long-term changes of different variables was tested using ordinary least-squares linear regressions. All statistical analyses were conducted in R v.4.0.2 (R Core Team, 2020).

2.2 Mesocosm experiment

2.2.1 Experimental design

A controlled experiment with *Lolium perenne* plants (my model grass species) was performed in a modernized version of the gas exchange mesocosm system described by Schnyder *et al.* (2003), which consisted of four plant growth chambers (PGR15, Conviron, Winnipeg, Canada). The experimental design was previously described in detail in Baca Cabrera *et al.* (2020): air temperature in the chambers was set to 20/16 °C during the

16 h/8 h, day/night cycle and a 3 × 2 factorial design was applied, with three c_a levels (200, 400 or 800 µmol mol^{-1} CO_2), corresponding to Last Glacial Maximum (half-ambient), present-day (ambient) and end of the century projections (elevated), and two daytime VPD levels (low = 0.59 kPa and high = 1.17 kPa), corresponding to dry or humid summer days in Central Europe. Air relative humidity (RH) was set to 50% (high VPD) or 75% (low VPD) during daytime and the photosynthetic photon flux density (PPFD) at canopy height was 800 µmol m^{-2} s^{-1}. Nighttime VPD was kept constant at 0.46 kPA (RH = 75%), for all treatments. The specified CO_2 concentration inside the chambers was obtained by mixing dry CO_2-free air and tank CO_2 (Linde AG, Unterschleißheim, Germany or CARBO Kohlensäurewerke, Bad Hönningen, Germany) using mass flow controllers. Air temperature and RH were controlled by the chamber control system (CMP6050, Conviron, Winnipeg, Canada).

Inside the growth chambers, individual *L. perenne* plants (cv. 'Acento') were placed in plastic tubes (350 mm height, 50 mm diameter) filled with washed quartz sand (0.3–0.8 mm grain size), at a density of 383 plants m^{-2}. This high density resulted in a canopy-like situation at harvest (leaf area index >5 after canopy closure, in all treatments), allowing a good approximation to conditions in the field. Plants were supplied with a modified 5 mM nitrate-N Hoagland nutrient solution every 6 h using the procedure described in Lehmeier *et al.* (2008): this corresponded to a nutrient solution with 33% reduced nitrate-N concentration relative to normal, and nominal concentrations of the other nutrients (compare to Kavanová *et al.*, 2008). A reduced N-concentration was selected to reproduce the conditions of nitrogen limitation often observed in terrestrial ecosystems, including grasslands (LeBauer & Treseder, 2008; Terrer *et al.*, 2019).

A total of five sequential experimental runs were performed, with a duration of 10–12 weeks per run. Treatment replicates were allocated to different chambers between sequential runs, to minimize potential chamber effects (Table 2.2). We observed no chamber effect on the parameters reported in this study.

Table 2.2: Experimental design of the *Lolium perenne* experiment, with a 3 x 2 experimental design: three c_a levels: 200, 400 or 800 µmol mol^{-1} CO_2 (C1, C2 or C3) and two VPD levels: high or low daytime VPD (**high** or **low**). Nighttime VPD was the same in all treatments. The treatment replicates were distributed between four growth chambers (no. 1–4).

	Treatment					
Run	C1/**high**	C2/**high**	C3/**high**	C1/**low**	C2/**low**	C3/**low**
	Chamber no.					
1st	1 / 2	3 / 4	-	-	-	-
2nd	-	1 / 2	3 / 4	-	-	-
3rd	-	-	-	3 / 4	1 / 2	-
4th	-	3	-	-	4	1 / 2
5th	3	-	1	2	-	4

2.2.2 Measurements performed

A broad spectrum of morphometric, physiological and isotopic measurements was performed during the mesocosm experiment after canopies were closed (leaf area index >5). These measurements were described in detail in Baca Cabrera *et al.* (2020) and Baca Cabrera *et al.* (2021b). Table 2.3 briefly summarizes the most relevant information about these measurements.

Table 2.3: Summary of all measurements performed in the mesocosm experiment

Parameter	Sample description	Method summary (reference)
Leaf elongation rate (LER)	Growing leaves of the main tiller of 16–40 plants per treatment (Runs I–IV, after canopy closure).	Distance between the tip of the elongating leaf and the ligule of the youngest fully expanded leaf was measured with a ruler at the end of the light period during 14 consecutive days (Schnyder & Nelson, 1988; Schnyder *et al.*, 1990).
LER_{day}, LER_{night}	Same as previous	Same method as for LER, but measurements were performed both at the end of the day and the night period, on two consecutive days
Morphometry (leaf length, leaf area, LAI)	16–40 plants per treatment (Runs I–IV, after LER measurements).	Plant fresh and dry weight were estimated gravimetrically and all tissues from the main tiller were photographed and analyzed digitally (Liu *et al.*, 2016).

Parameter	Sample description	Method summary (reference)
Epidermal cell length and number	Two fully developed leaf blades from four plants per treatment (Runs III–V, after LER measurements).	Leaves were cut near the ligule and 3 cm-long replicas of the abaxial epidermis were taken in the basal region, photographed with a fluorescence microscope (CALM, TUM) and analyzed digitally (Schnyder *et al.*, 1990).
Leaf-scale gas exchange (A_{leaf}, E_{leaf}, g_s)	Youngest fully developed leaf blade of four tillers of 6–12 plants per treatment (Runs I–V, after canopy closure).	Mid-sections of leaves were placed in a clamp-on leaf cuvette and CO_2 and H_2O exchange measured with an IRGA. CO_2 and VPD conditions in the cuvette were kept the same as in the growth environment (Baca Cabrera *et al.*, 2020).
Canopy-scale gas exchange (A_{canopy}, E_{canopy}, g_{canopy})	Closed canopies were measured under steady-state conditions (Runs I–IV, after canopy closure).	Air flow rate and CO_2 and H_2O concentration were measured at chamber inlet and outlet every 30 minutes with an IRGA, during a two-week interval (Baca Cabrera *et al.*, 2020).
Water-soluble carbohydrates (WSC)	Leaf growth-and-differentiation zones (LGDZ) from two mature tillers of six plants per chamber (Runs I–IV, after canopy closure).	Samples were taken at the end of the day and the night period, pooled by sampling time (n=4 per treatment and period), frozen and stored until WSC extraction and quantification as in Schnyder & de Visser (1999) and Baca Cabrera *et al.* (2020).
Osmotic potential	Same samples as for the previous parameter (Run V).	Sap from thawed samples was extracted with mechanical pressure and osmotic potential measured with a vapor pressure osmometer (Baca Cabrera *et al.*, 2020).
Leaf water potential	Youngest fully expanded leaf blade of 8 plants per treatment (Run V, after canopy closure).	Leaf blades were cut near the ligule and immediately placed in a pressure chamber, following the recommendations by Turner (1981). Measurements were performed at the end of the day and night periods.
Turgor	Calculated parameter	Turgor was estimated as the difference between osmotic and leaf water potential (Baca Cabrera *et al.*, 2020).
$\delta^{18}O$ of tissue water	LGDZ and two youngest fully developed leaf blades of three mature tillers of 12	Samples were taken at the end of the day and the night period, pooled into two subsamples and frozen until water extraction. Tissue water was extracted by cryogenic distillation and $\delta^{18}O$

Parameter	Sample description	Method summary (reference)
	plants per chamber (Runs I–V, after canopy closure).	analyzed by cavity ring-down spectroscopy (Liu *et al.*, 2016).
$\delta^{18}O$ of leaf cellulose and sucrose	Two youngest fully developed leaf blades of two mature tillers of twelve plants per chamber (Runs I–V, after canopy closure).	Samples were taken at the end of the day and the night period, pooled into two subsamples and frozen until extraction. α-cellulose was extracted as in Gaudinski *et al.* (2005) and sucrose was separated by HPLC as in Gebbing & Schnyder (2001). Samples were measured by IRMS (Baca Cabrera *et al.*, 2021a).
N-concentration in leaf blades	Same as previous parameter	N elemental concentration of the samples was measured by IRMS (Baca Cabrera *et al.*, 2021a).

2.2.3 Statistical analysis

The statistical methods used for this research have been described in detail in Baca Cabrera *et al.* (2020) and Baca Cabrera *et al.* (2021b). Briefly, I tested the effect of CO_2, VPD and their interactions on all parameters described in Table 2.3, including the differences between day and night period, when needed. For this, two main statistical methods were used: (1) linear mixed models, with the individual target parameters defined as the *fixed effect* and canopy, experimental run and multiple measurements on individual plants defined as the *random effects*; and (2) two-way ANOVA tests, using canopy-scale averages for each individual treatment as replicates (n = 2–5, depending on treatment and target parameter). Additionally, ordinary least-squares linear regressions were performed to test the relationship between the different target variables (using treatment averages). All statistical analyses were performed in R v.4.0.2 (R Core Team, 2020).

2.3 $\delta^{18}O_{cellulose}$ process-chain

To address the uncertainties in the process-chain determining $\delta^{18}O_{cellulose}$ of grassland vegetation, a controlled experiment with perennial ryegrass and simulations of a temperate grassland were performed. Here, I briefly summarize the methods used:

Controlled experiment

The $\delta^{18}O$ study was performed as part of the *L. perenne* mesocosm experiment described in Section 2.2. The main purpose of this experiment was to track the ^{18}O signal from source water to cellulose in *L. perenne* plants under contrasting c_a (half-ambient, ambient and

elevated) and VPD (low and high) levels (Baca Cabrera *et al.*, 2021b). For this, fully developed leaf blades and leaf growth-and-differentiation zones (LGDZ) were sampled after canopy closure (see Table 2.3 for details about the sample size) and $\delta^{18}O$ was measured in the following compartments: tissue water of leaf blades ($\delta^{18}O_{LW}$) and of the LGDZ (designated $\delta^{18}O_{CelSynW}$, with CelSynW designating the water at the site of cellulose synthesis in the LGDZ); and cellulose and sucrose of leaf blades ($\delta^{18}O_{cellulose}$ and $\delta^{18}O_{sucrose}$). Tissue water was extracted using cryogenic distillation and analyzed by cavity ring-down spectroscopy as in Liu *et al.* (2016). α-cellulose was extracted with the Brendel *et al.* (2000) protocol as modified by Gaudinski *et al.* (2005) and sucrose was separated by preparative HPLC as in Gebbing & Schnyder (2001). Sucrose and cellulose samples were analyzed by isotope ratio mass spectrometry as in Baca Cabrera *et al.* (2021a).

Additionally, the ^{18}O-enrichment above source water ($\Delta^{18}O$) was estimated for all compartments, based on the $\delta^{18}O$ of the nutrient solution (equated with the water taken up by the plants, see Liu *et al.*, 2017), which was constant throughout the experiment, and the ^{18}O-enrichment of water at the site of sucrose synthesis ($\Delta^{18}O_{SucSynW}$), calculated as $\Delta^{18}O_{Sucrose} - \varepsilon_{bio}$. By comparing $\Delta^{18}O_{SucSynW}$ and $\Delta^{18}O_{LW}$ in all treatments, the presence of isotopic gradients and the effect of c_a and VPD on these gradients could be tested. Finally, the attenuation factor $p_{ex}p_x$ – that gives the proportion of post-photosynthetically exchanged oxygen in cellulose – was calculated based on the Barbour & Farquhar (2000) model (Eqn 1.3). $p_{ex}p_x$ was referenced alternatively to ^{18}O-enrichment of sucrose synthesis water ($p_{ex}p_{x\text{-}SucSynW}$) or of bulk leaf water ($p_{ex}p_{x\text{-}LW}$).

Process-based modelling with MuSICA

The isotope-enabled soil–vegetation–atmosphere transfer model MuSICA (Ogée *et al.*, 2003; Ogée *et al.*, 2007) was applied to simulate ecosystem CO_2, energy and water fluxes and the ^{18}O composition of various ecosystem compartments in a temperate humid grassland at the former Grünschwaige Grassland Research Station of TUM (see Schnyder *et al.*, 2006 for details on the site and management). In a first step, the model was parametrized for the study site to track the $\delta^{18}O$ dynamics of water pools from the soil to the leaves (Hirl *et al.*, 2019) and, in a second step, an allocation-and-growth module was developed to predict the $\delta^{18}O$ dynamics in sugar and cellulose pools (Hirl *et al.*, 2021). The model was forced by half-hourly meteorological and isotopic input data ($\delta^{18}O$ of rainwater and water vapor) for the period 2006–2012 and applied to predict key physiological parameters such as canopy-scale photosynthesis, transpiration and stomatal conductance and the ^{18}O composition of source water (the water taken up by plants), leaf water, leaf sucrose and leaf cellulose. The CO_2 and water fluxes were validated against eddy-flux

measurements, and predictions of $\delta^{18}O$ of source water, leaf water and leaf cellulose were compared with observations from samples collected at noon over biweekly intervals during the vegetation periods of seven years (2006-2012). Observations included soil water at two depths (7 and 20 cm), stem water, leaf water and leaf cellulose of mixed-species samples of the co-dominant members of the grassland community. $\delta^{18}O_{LW}$ was measured by cavity ring-down spectroscopy (Liu *et al.*, 2016) and $\delta^{18}O_{cellulose}$ by isotope ratio mass spectrometry (Hirl *et al.*, 2019).

The use of MuSICA contributed to the findings of this thesis principally in two ways: (1) it predicted the relationship between canopy stomatal conductance and $\delta^{18}O_{cellulose}$ (or its enrichment above source water, $\Delta^{18}O_{cellulose}$) of a C_3 grassland under natural conditions; and (2) it estimated the response of the attenuation factor $p_{ex}p_x$ and ε_{bio} to varying environmental conditions by means of a sensitivity analysis.

3. Summaries of manuscripts and author contributions

This thesis consists of two first-author and two co-author published papers, and one first-author unpublished manuscript, available as a preprint. The abstracts and the authors' contributions are given below. All publications resulted from the DFG project SCHN 557/9-1: "The significance of cellulose-$\delta^{18}O$ for understanding water-use efficiency of grassland: Evidence from experimental, observational and process-based modeling studies".

3.1 Publication 1: Stomatal conductance limited the CO_2 response of grassland in the last century

Juan C Baca Cabrera, Regina T Hirl, Rudi Schäufele, Andy Macdonald, Hans Schnyder

Published in BMC Biology: 19, 50, 2021. doi: 10.1186/s12915-021-00988-4

Abstract

The anthropogenic increase of atmospheric CO_2 concentration (c_a) is impacting carbon (C), water, and nitrogen (N) cycles in grassland. Plant canopy stomatal conductance is a key player in these coupled cycles: it is a physiological control of vegetation water-use efficiency (the ratio of C gain by photosynthesis to water loss by transpiration), and it responds to photosynthetic activity, which is influenced by vegetation N status. It is unknown if the c_a-increase and climate change over the last century have already affected canopy stomatal conductance and its links with C and N processes in grassland. Here, we assessed two independent proxies of stomatal conductance changes over the last century: trends of $\delta^{18}O$ in cellulose ($\delta^{18}O_{cellulose}$) in archived herbage from a wide range of grassland communities on the Park Grass Experiment at Rothamsted (U.K.) and changes of the ratio of yields to the CO_2 concentration gradient between the atmosphere and the leaf internal gas space ($c_a - c_i$). The two proxies correlated closely ($R^2 = 0.70$). In addition, the sensitivity of $\delta^{18}O_{cellulose}$ changes to estimated stomatal conductance changes agreed broadly with published sensitivities across a range of contemporary field and controlled environment studies, further supporting the utility of $\delta^{18}O_{cellulose}$ changes for historical reconstruction of stomatal conductance changes at Park Grass. Trends of $\delta^{18}O_{cellulose}$ differed strongly between plots and indicated much greater reductions of stomatal conductance in grass-rich than dicot-rich communities. Reductions of stomatal conductance were connected with reductions of yield trends, nitrogen acquisition, and nitrogen nutrition index. Although all plots were nitrogen-limited or phosphorus- and nitrogen-co-limited to different degrees, long-term reductions of stomatal conductance were largely independent of fertilizer regimes and soil pH, except for nitrogen fertilizer supply which promoted the abundance of grasses. Our data indicate that some types of temperate grassland may have attained saturation of C sink activity more than one century ago. Increasing N fertilizer supply may not be an effective climate change mitigation strategy in many grasslands, as it promotes the expansion of grasses at the disadvantage of the more CO_2 responsive forbs and N-fixing legumes

Contributions

JCBC and HS designed the study. AM guided the sampling in the Rothamsted archive. RS performed the carbon and oxygen isotope and carbon and nitrogen elemental analyses. RTH performed the phosphorus analyses. JCBC analyzed all data. JCBC and HS interpreted the data and wrote the manuscript. All authors contributed to the revision of the manuscript.

3.2 Publication 2: Atmospheric CO_2 and VPD alter the diel oscillation of leaf elongation in perennial ryegrass: compensation of hydraulic limitation by stored-growth

Juan C Baca Cabrera, Regina T Hirl, Jianjun Zhu, Rudi Schäufele, Hans Schnyder

Published in New Phytologist: 227, 1776–1789, 2020. doi: 10.1111/nph.16639

Abstract

We explored the effects of atmospheric CO_2 concentration (C_a) and vapor pressure deficit (VPD) on putative mechanisms controlling leaf elongation in perennial ryegrass. Plants were grown in stands at a C_a of 200, 400 or 800 µmol mol^{-1} combined with high (1.17 kPa) or low (0.59 kPa) VPD during the 16 h-day in well-watered conditions with reduced nitrogen supply. We measured day : night-variation of leaf elongation rate (LER_{day} : LER_{night}), final leaf length and width, epidermal cell number and length, stomatal conductance, transpiration, leaf water potential and water-soluble carbohydrates and osmotic potential in the leaf growth-and-differentiation zone (LGDZ). Daily mean LER or morphometric parameters did not differ between treatments, but LER_{night} strongly exceeded LER_{day}, particularly at low C_a and high VPD. Across treatments LER_{day} was negatively related to transpiration (R^2 = 0.75) and leaf water potential (R^2 = 0.81), while LER_{night} was independent of leaf water potential or turgor. Enhancement of LER_{night} over LER_{day} was proportional to the turgor-change between day and night (R^2 = 0.93). LGDZ sugar concentration was high throughout diel cycles, providing no evidence of source limitation in any treatment. Our data indicate a mechanism of diel cycling between daytime hydraulic and nighttime stored-growth controls of LER, buffering C_a and daytime VPD effects on leaf elongation.

Contributions

JCBC and HS designed the experiment. JCBC performed the research, analyzed the data and wrote the first draft. RTH, JZ and RS helped with gas exchange measurements. All authors contributed to the revision of the manuscript.

3.3 Publication 3: ^{18}O enrichment of leaf cellulose correlated with ^{18}O enrichment of leaf sucrose but not bulk leaf water in a C_3 grass across contrasts of atmospheric CO_2 concentration and air humidity

Juan C Baca Cabrera, Regina T Hirl, Rudi Schäufele, Jianjun Zhu, Haitao Liu, Jérôme Ogée, Hans Schnyder

Preprint available, doi: 10.21203/rs.3.rs-596094/v1

Abstract

The ^{18}O composition of plant cellulose is often used to reconstruct past climate and plant function. However, uncertainty remains regarding the estimation of the leaf sucrose ^{18}O signal and its subsequent attenuation by ^{18}O exchange with source water during cellulose synthesis. We grew *Lolium perenne* at three CO_2 concentrations (200, 400 or 800 μmol mol^{-1}) and two relative humidity (RH) levels (50% or 75%), and determined ^{18}O enrichment of leaf sucrose ($\Delta^{18}O_{Sucrose}$), bulk leaf water ($\Delta^{18}O_{LW}$), leaf cellulose ($\Delta^{18}O_{Cellulose}$) and water at the site of cellulose synthesis ($\Delta^{18}O_{CelSynW}$). $\Delta^{18}O_{Cellulose}$ correlated with $\Delta^{18}O_{Sucrose}$ (R^2 = 0.87) but not with $\Delta^{18}O_{LW}$ (R^2 = 0.04), due to a variable ^{18}O discrepancy (range 2.0–9.0‰) between sucrose synthesis water ($\Delta^{18}O_{SucSynW}$, estimated from $\Delta^{18}O_{Sucrose}$) and bulk leaf water. The discrepancy resulted mainly from an RH effect. The proportion of oxygen in cellulose that exchanged with medium water during cellulose formation (p_{ex}), was near-constant when referenced to $\Delta^{18}O_{SucSynW}$ ($p_{ex\text{-}SucSynW}$ = 0.52 ± 0.02 SE), but varied when related to bulk leaf water ($p_{ex\text{-}LW}$ = −0.01 to 0.46). We conclude that previously reported RH-dependent variations of $p_{ex\text{-}LW}$ in grasses are related to a discrepancy between $\Delta^{18}O_{SucSynW}$ and $\Delta^{18}O_{LW}$ that may result from spatial heterogeneity in ^{18}O gradients of leaf water and photosynthetic sucrose synthesis.

Contributions

HS, JCBC and RTH designed the study. JCBC, RTH and JZ performed the experiments, sampling, and sample processing. RS performed the isotope analyses. JCBC analyzed the data and wrote the first draft. JCBC, HS, JO, RTH, RS, JZ and HL contributed to the discussion and revision of the manuscript.

3.4 Publication 4: The ^{18}O ecohydrology of a grassland ecosystem – predictions and observations

Regina T Hirl, Hans Schnyder, Ulrike Ostler, Rudi Schäufele, Inga Schleip, Sylvia H Vetter, Karl Auerswald, Juan C Baca Cabrera, Lisa Wingate, Margaret M Barbour, Jérôme Ogée

Published in Hydrology and Earth System Sciences: 23, 2581–2600, 2019. doi: 10.5194/hess-23-2581-2019

Abstract

The oxygen isotope composition ($\delta^{18}O$) of leaf water ($\delta^{18}O_{leaf}$) is an important determinant of environmental and physiological information found in biological archives, but the system-scale understanding of the propagation of the $\delta^{18}O$ of rain through soil and xylem water to $\delta^{18}O_{leaf}$ has not been verified for grassland. Here we report a unique and comprehensive dataset of fortnightly $\delta^{18}O$ observations in soil, stem and leaf waters made over seven growing seasons in a temperate, drought-prone, mixed-species grassland. Using the ecohydrology part of a physically based, ^{18}O-enabled soil–plant–atmosphere transfer model (MuSICA), we evaluated our ability to predict the dynamics of $\delta^{18}O$ in soil water, the depth of water uptake, and the effects of soil and atmospheric moisture on ^{18}O enrichment of leaf water ($\Delta^{18}O_{leaf}$) in this ecosystem. The model accurately predicted the $\delta^{18}O$ dynamics of the different ecosystem water pools, suggesting that the model generated realistic predictions of the vertical distribution of soil water and root water uptake dynamics. Observations and model predictions indicated that water uptake occurred predominantly from shallow (<20 cm) soil depths throughout dry and wet periods in all years, presumably due (at least in part) to the effects of high grazing pressure on root system turnover and placement. $\Delta^{18}O_{leaf}$ responded to both soil and atmospheric moisture contents and was best described in terms of constant proportions of unenriched and evaporatively enriched water (two-pool model). The good agreement between model predictions and observations is remarkable as model parameters describing the relevant physical features or functional relationships of soil and vegetation were held constant with one single value for the entire mixed-species ecosystem.

Contributions

JO, RTH and HS designed the study. RTH analyzed the data and performed the modelling with guidance by JO. IS and UO designed the sampling scheme and setup, tested the water extraction unit and performed the diurnal water sampling. RS performed the isotope analysis. SHV analyzed the eddy flux data. MMB performed the supplementary controlled environment experiments. RTH and HS wrote the paper. RTH, HS, UO, RS, IS, SHV, KA, JCBC, LA, MMB and JO contributed to the discussion and revision of the manuscript.

3.5 Publication 5: Temperature-sensitive biochemical ^{18}O-fractionation and humidity-dependent attenuation factor are needed to predict $\delta^{18}O$ of cellulose from leaf water in a grassland ecosystem

Regina T Hirl, Jérôme Ogée, Ulrike Ostler, Rudi Schäufele, Juan C Baca Cabrera, Jianjun Zhu, Inga Schleip, Lisa Wingate, Hans Schnyder

Published in New Phytologist: 229, 3156–3171, 2019. doi: 10.1111/nph.17111

Abstract

We explore here our mechanistic understanding of the environmental and physiological processes that determine the oxygen isotope composition of leaf cellulose ($\delta^{18}O_{cellulose}$) in a drought-prone, temperate grassland ecosystem. A new allocation-and-growth model was designed and added to an ^{18}O-enabled soil–vegetation–atmosphere transfer model (MuSICA) to predict seasonal (April–October) and multi-annual (2007–2012) variation of $\delta^{18}O_{cellulose}$ and ^{18}O-enrichment of leaf cellulose ($\Delta^{18}O_{cellulose}$) based on the Barbour–Farquhar model. Modelled $\delta^{18}O_{cellulose}$ agreed best with observations when integrated over c. 400 growing-degree-days, similar to the average leaf lifespan observed at the site. Over the integration time, air temperature ranged from 7 to 22°C and midday relative humidity from 47 to 73%. Model agreement with observations of $\delta^{18}O_{cellulose}$ (R^2 = 0.57) and $\Delta^{18}O_{cellulose}$ (R^2 = 0.74), and their negative relationship with canopy conductance, was improved significantly when both the biochemical ^{18}O-fractionation between water and substrate for cellulose synthesis (ε_{bio}, range 26–30‰) was temperature-sensitive, as previously reported for aquatic plants and heterotrophically grown wheat seedlings, and the proportion of oxygen in cellulose reflecting leaf water ^{18}O-enrichment ($1 - p_{ex}p_x$, range 0.23–0.63) was dependent on air relative humidity, as observed in independent controlled experiments with grasses. Understanding physiological information in $\delta^{18}O_{cellulose}$ requires quantitative knowledge of climatic effects on $p_{ex}p_x$ and ε_{bio}.

Contributions

RTH, JO and HS designed the research. RTH, UO and HS designed the allocation-and-growth model. RTH analyzed the data and performed the modelling with guidance by JO and UO. RS performed the isotope analysis. HS, UO and IS designed and UO and IS performed the tracer experiment. HS and RTH planned and RTH, JCBC and JZ performed the mesocosm experiment. RTH wrote the first draft. RTH, JO, UO, RS, JCBC, JZ, IS, LW and HS contributed to the discussion and the revision of the manuscript.

4. Summarizing discussion

4.1 Consistent decrease of stomatal conductance in grassland vegetation under rising c_a and VPD

This thesis examined the response of stomatal conductance of C_3 grassland vegetation to parameters of global change at different scales. In a first step, the century-scale response of stomatal conductance at Park Grass was assessed by means of elemental and isotopic analyses of archived herbage samples (Baca Cabrera *et al.*, 2021a). Two independent indicators of stomatal conductance change were used: changes of $\delta^{18}O_{cellulose}$ in plant biomass and yield-based stomatal conductance ($g_{s\ yield}$), estimated from herbage yield and $\delta^{13}C$ of bulk biomass (Materials and Methods). In a second step, the stomatal conductance response of a model C_3 grass species, *L. perenne*, to c_a and VPD was investigated in controlled environment conditions (Baca Cabrera *et al.*, 2020).

At Park Grass, $\delta^{18}O_{cellulose}$ significantly increased over the last century on average of all treatments (+0.7‰, $P < 0.001$). $\delta^{18}O_{cellulose}$ increases are indicative of decreases of stomatal conductance, under otherwise equal environmental conditions (Farquhar *et al.*, 1998; Barbour *et al.*, 2000; and see Section 4.3), including rainfall, atmospheric humidity, vapor pressure deficit and isotopic inputs of rain ($\delta^{18}O_{rain}$). I found no evidence of significant trends of these latter variables at Park Grass during spring growth, despite a large increase in daily mean temperature (Table 4.1a), indicating that the observed long-term changes in $\delta^{18}O_{cellulose}$ were not associated with changes in meteorological conditions. Most interestingly, the increase of $\delta^{18}O_{cellulose}$ was significantly greater in grass-rich than dicot-rich communities (Fig. 4.1a, Table 4.1b), hinting to a greater c_a-sensitivity of grasses in terms of their long-term stomatal conductance response compared with that of forbs and legumes. Long-term decreases in stomatal conductance at Park Grass were also suggested by strong average decreases in $g_{s\ yield}$ during the last 100 years (average −29.5%, $P < 0.001$). Again, that decrease was significantly more pronounced in grass-rich than in dicot-rich communities (Fig. 4.1b, Table 4.1b), also supporting a stronger stomatal conductance sensitivity of grasses compared with other functional groups, a response that was also observed in FACE experiments that explore plant responses to future elevated CO_2 conditions (Ainsworth & Rogers, 2007).

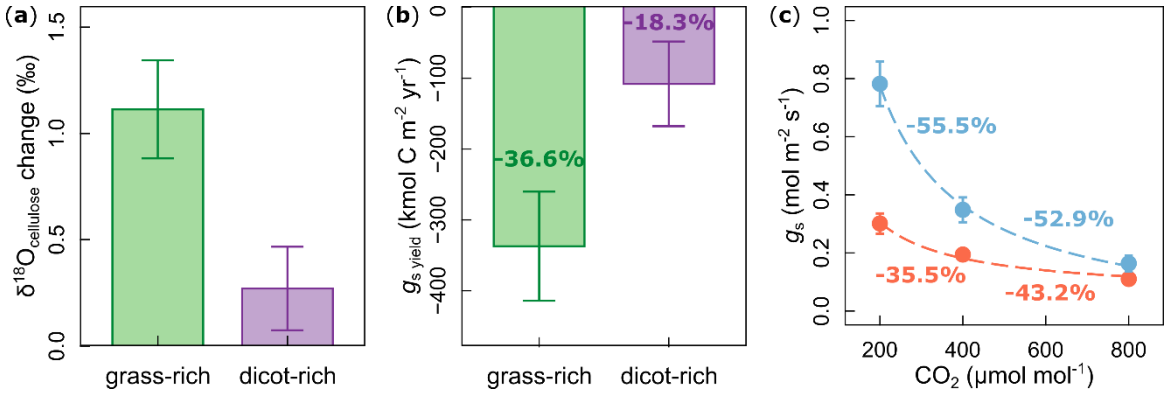

Fig. 4.1: Stomatal conductance response to atmospheric CO_2 concentration and vapor pressure deficit. Long-term changes in $\delta^{18}O_{cellulose}$ (**a**) and of canopy-scale, growing season-integrated stomatal conductance ($g_{s\ yield}$) (**b**) in grass-rich (green) and dicot-rich (violet) communities at Park Grass, calculated as the difference between 15-year periods at the end (2004–2018) and the beginning (1917–1931) of the last century; and stomatal conductance (g_s) of the youngest fully-expanded leaf of *L. perenne* as affected by atmospheric CO_2 concentration and vapor pressure deficit (VPD) (low VPD = blue, high VPD = red) during growth in controlled environment mesocosms (**c**). Values in (**b**) express the %-$g_{s\ yield}$ decrease during the last century (c_a increased from c. 300 to c. 400 µmol mol^{-1} during that time span) at Park Grass; and values in (**c**) express the %-g_s decrease between CO_2 levels in the mesocosms. Data points and error bars represent the mean ± SE. The dashed lines in (**c**) represent significant regressions. (**a**) and (**b**) adapted from Baca Cabrera *et al.* (2021a); (**c**) adapted from Baca Cabrera *et al.* (2020).

Table 4.1: Long-term meteorological and physiological trends at Park Grass. (**a**): 15-year averages (mean ± SE) of meteorological variables at the beginning (1917–1931) and at the end (2004–2018) of the last century during spring growth and results of the Mann-Kendal trend test for the last 100 years. And, (**b**): results of t-tests of the difference (mean ± SE) between 15-year periods at the end (2004–2018) and the beginning (1917–1931) of the last century during spring growth for multiple physiological parameters. t-test results are presented for all fertilizer treatments combined (n = 12), for grass-rich (n = 6) and dicot-rich communities (n = 6), and for the difference between grass-rich and dicot-rich treatments. Significance levels: ns, not significant (P > 0.05); *****, P < 0.05; ******, P < 0.01; *******, P < 0.001.

(**a**)	Trends in meteorological conditions		
Parameter	1917–1931	2004–2018	Mann-Kendal test (1917–2018)
Mean temperature (°C)	10.7 ± 0.1	12.2 ± 0.2	P < 0.001
VPD (kPa)	0.37 ± 0.02	0.41 ± 0.02	P = 0.79
Relative humidity (%)	74.6 ± 0.8	73.3 ± 0.9	P = 0.13
Precipitation (mm)	163.7 ± 12.3	162.2 ± 18.3	P = 0.73

(**b**)	Long-term changes in grassland vegetation			
Parameter	All treatments	Grass-rich	Dicot-rich	Grass vs. dicot
$\delta^{18}O_{cellulose}$ change (‰)	+0.7 ± 0.2***	+1.1 ± 0.2***	+0.3 ± 0.2^{ns}	***

$g_{s\ yield}$ change (kmol C m^{-2} yr^{-1})	−225 ± 52***	−339 ± 77***	−110 ± 60*	***
Yield change (g m^{-2})	−35 ± 29^{ns}	−78 ± 42*	+8.6 ± 33^{ns}	***
WUE_i change (μmol mol^{-1})	+9.6 ± 0.6***	+10.9 ± 0.9***	+8.2 ± 0.5***	***
c_i/c_a change	−0.004 ± 0.003^{ns}	−0.008 ± 0.004**	+0.001 ± 0.002^{ns}	***
N acquisition change (g m^{-2})	−1.1 ± 0.5**	−1.9 ± 0.7***	−0.3 ± 0.5^{ns}	***
NNI change	−0.06 ± 0.02***	−0.08 ± 0.02***	−0.04 ± 0.02*	**

The large stomatal conductance decrease observed in plant communities at Park Grass was associated mainly (or completely) with the increase of c_a during the last 100 years, as vapor pressure deficit or relative humidity did not change significantly during this period. The effect of c_a on stomatal conductance was also evidenced in the *L. perenne* experiment in controlled environment conditions. Stomatal conductance significantly decreased under rising c_a (Fig. 4.1c, Table 4.2), showing a strong nonlinear response, as expected from theoretical considerations and modelling (Katul *et al.*, 2010; Buckley & Schymanski, 2014; Dewar *et al.*, 2018) and empirical knowledge (Yu *et al.*, 2004). Interestingly, the %-decrease in stomatal conductance between half-ambient and ambient c_a was very similar to that between ambient and elevated c_a, indicating that stomatal conductance changes of grasslands registered in the past (e.g. at Park Grass) could potentially be used to predict their behavior at the end of the 21th century, if c_a indeed rises to 800 μmol mol^{-1}. Furthermore, stomatal conductance was clearly higher at low VPD at all c_a levels and a significant interaction between c_a and VPD was also observed (Table 4.2): the enhancement of stomatal conductance by low VPD (relative to high VPD) was greater at a c_a of 200 μmol mol^{-1} (2.6-fold) than at 800 μmol mol^{-1} (1.5-fold) (Fig. 4.1c). The data suggest that there was a gradual shift in stomatal regulation from maximization of carbon gain at half-ambient c_a to minimization of water loss at elevated c_a, which would agree with the formulation by Katul *et al.* (2010) that the cost of unit water loss increases under rising c_a (but see Medlyn *et al.*, 2013; Buckley & Schymanski, 2014). However, investigations with more species and under a broader array of environmental conditions (e.g. drought stress) would be needed to address this in detail.

Table 4.2: Effect of CO_2, VPD and their interaction on physiological parameters of *L. perenne*. Average value across treatments (mean ± SE) and total range (minimum and maximum treatment means) for multiple physiological parameters measured in the mesocosm experiment (see Baca Cabrera *et al.*, 2020; Baca Cabrera *et al.*, 2021b for details about the replicate number). Significance levels: ns, not significant ($P > 0.05$); *****, $P < 0.05$; ******, $P < 0.01$; *******, $P < 0.001$.

Parameter	Average across treatments	Total range	Significance		
			CO_2	VPD	CO_2 : VPD
g_s (day) (mol m^{-2} s^{-1})	0.32 ± 0.10	0.11 – 0.78	*******	*******	*******
A_{leaf} (µmol m^{-2} s^{-1})	10.7 ± 0.6	8.6 – 12.7	ns	ns	ns
E_{leaf} (day) (mmol m^{-2} s^{-1})	2.1 ± 0.4	1.0 – 3.3	*******	ns	ns
$WUE_{i\ leaf}$ (day) (µmol mol^{-1})	57.4 ± 16.5	12.9 – 123.5	***	******	**
WUE_{leaf} (day) (mmol mol^{-1})	6.6 ± 1.6	2.6 – 12.8	***	*******	ns
LER (mm h^{-1})	0.96 ± 0.01	0.94 – 0.99	ns	ns	ns
LER_{day} (mm h^{-1})	0.82 ± 0.03	0.70 – 0.88	*	ns	*
LER_{night} (mm h^{-1})	1.26 ± 0.05	1.12 – 1.45	*	ns	ns
Cell length (mm)	0.82 ± 0.01	0.79 – 0.89	ns	ns	ns
Leaf length (cm)	27.3 ± 0.7	24.6 – 29.1	ns	ns	ns
Leaf width (mm)	3.5 ± 0.1	3.3 – 3.6	ns	ns	ns
Leaf water potential (day) (MPa)	-1.5 ± 0.2	−1.9 – −1.1	***	*******	ns
Leaf water potential (night) (MPa)	-0.6 ± 0.02	−0.6 – −0.7	ns	ns	ns
Turgor (day) (MPa)	0.6 ± 0.06	0.4 – 0.7	*	ns	ns
Turgor (night) (MPa)	1.1 ± 0.03	1.1 – 1.2	ns	ns	ns
NNI	0.49 ± 0.04	0.34 – 0.79	***	*	ns
$\Delta^{18}O_{LW}$ (day) (‰)	9.2 ± 0.4	7.9 –10.2	**	ns	ns
$\Delta^{18}O_{LW}$ (night) (‰)	8.1 ± 0.3	6.7 – 8.8	***	ns	ns
$\Delta^{18}O_{sucrose}$ (day) (‰)	41.5 ± 1.6	37.4 – 46.3	ns	***	ns
$\Delta^{18}O_{sucrose}$ (night) (‰)	40.9 ± 1.5	36.6 – 45.7	*	***	ns
$\Delta^{18}O_{SucSynW} - \Delta^{18}O_{LW}$ (‰)	5.3 ± 1.4	2.0 – 9.0	ns	***	ns
$\Delta^{18}O_{CelSynW}$ (‰)	0.48 ± 0.09	0.14 – 0.83	*	ns	ns
$p_{x\text{-}LW}$	0.95 ± 0.01	0.92 – 0.99	ns	ns	ns
$p_{x\text{-}SucSynW}$	0.97 ± 0.01	0.93 – 0.99	ns	**	ns
$\Delta^{18}O_{Cellulose}$ (‰)	33.8 ± 0.7	32.2 – 35.7	ns	***	ns
$p_{ex\text{-}LW}$	0.24 ± 0.08	−0.01 – 0.46	*	***	ns
$p_{ex\text{-}SucSynW}$	0.52 ± 0.02	0.47 – 0.58	ns	ns	ns

The results presented here showed a consistent decrease of stomatal conductance of grassland vegetation under rising c_a. Large decreases associated with the anthropogenic c_a increase have already occurred in the past, as evidenced from the Park

Grass long-term changes and the response of *L*. *perenne* at half-ambient c_a, and will probably continue in the future, as shown by the stomatal closure of C_3 grasses at elevated c_a reported here, which is in agreement with observations from FACE experiments (Ainsworth & Rogers, 2007; Kimball, 2016). Also, it was shown that the magnitude of the stomatal conductance response of grassland vegetation to elevated c_a will depend on at least two additional factors: (1) future changes in VPD, a factor that negatively affects stomatal conductance and that strongly interacts with c_a; and (2) the community composition of grasslands, with grass-rich communities showing a significantly larger response to c_a than dicot-rich (forbs, legumes) communities. In the next section, I discuss how the observed stomatal conductance responses affected other key physiologic parameters and the resulting implications.

4.2 Effects of stomatal conductance changes in grassland vegetation under N-limiting conditions

4.2.1 Stomatal conductance limits the CO_2 response at Park Grass

At Park Grass, intrinsic water-use efficiency had the most robust long-term response among the parameters investigated, showing a significant increase in all fertilizer treatments during the last century, which is consistent with the positive response of intrinsic water-use efficiency to c_a commonly observed in FACE experiments (Leakey *et al.*, 2019). On average, intrinsic water-use efficiency was +9.6 µmol mol^{-1} or c. 31% higher than a century ago (Fig. 4.2a, $P < 0.001$), but the increase of intrinsic water-use efficiency was c. 33% greater in the grass-rich swards compared to dicot-rich plant communities.

Remarkably, the increase in intrinsic water-use efficiency was not coupled with an increase in herbage yield trends. Overall, there was no significant long-term change in yield at Park Grass (Table 4.1b) and the trends diverged for the dicot- and grass-rich treatments ($P < 0.001$). While the yields of the grass-rich treatments decreased by 16% on average during the last 100 years, yield trends of the dicot-rich plots were not significant, aligning with the previous observation that annual yields of the Park Grass plots have not increased systematically in the 20th century (Jenkinson *et al.*, 1994). Assuming herbage yield is a proxy for growing-season integrated canopy photosynthesis (see Baca Cabrera *et al.*, 2021a), then it can be concluded that the long-term increase in intrinsic water-use efficiency at Park Grass was mainly caused by the reported decrease in stomatal conductance, rather than by an enhancement of net photosynthesis, indicating a limited or no or – counterintuitively – perhaps even a negative carbon fertilization effect. Indeed, $\delta^{18}O_{cellulose}$ trends were significantly related with intrinsic water-use efficiency

trends (positive relationship, $P < 0.05$) and with yield trends (negative relationship, $P < 0.01$) (Fig. 4.2d,e), pointing to stomatal conductance (integrated over the growing season and canopy) as the likely primary control of treatment-dependent trends of intrinsic water-use efficiency and yields in the last century.

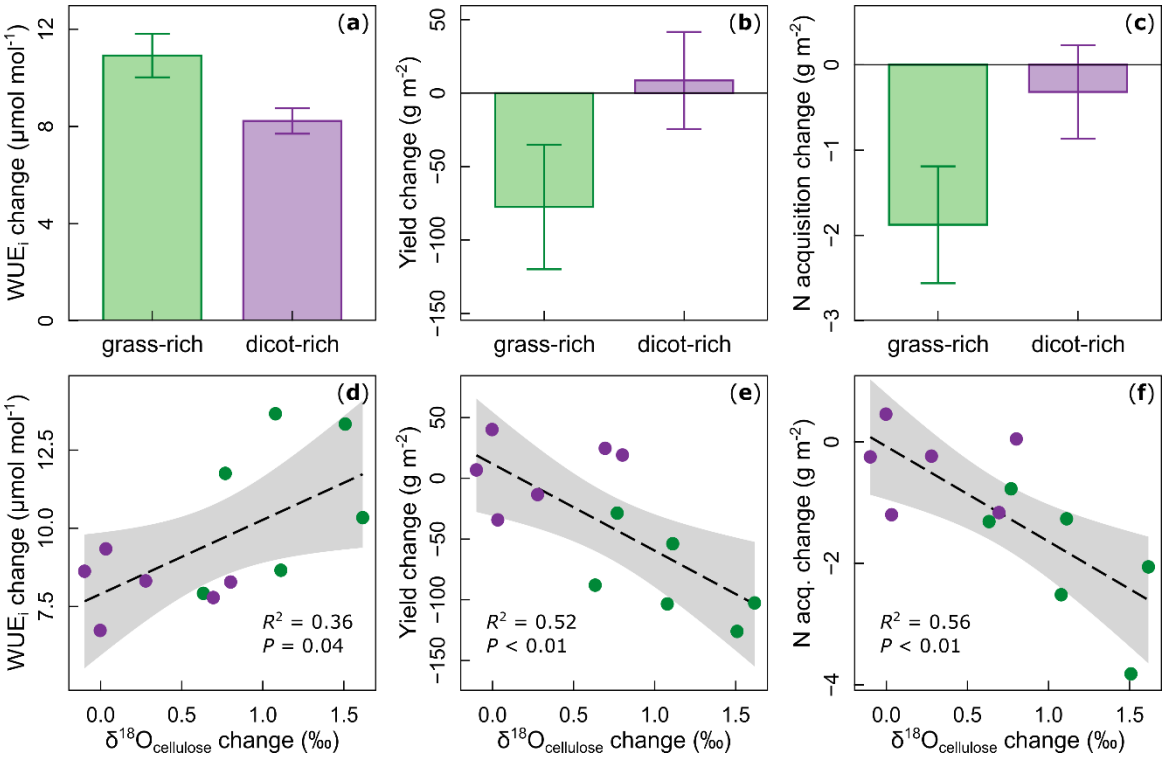

Fig. 4.2: Long-term physiological responses at Park Grass. Long-term changes in intrinsic water-use efficiency (WUE_i) (**a**), herbage yield (**b**) and N acquisition (**c**); and relationship between long-term changes in $\delta^{18}O_{cellulose}$ and long-term changes in WUE_i (**d**), herbage yield (**e**) and nitrogen acquisition (**f**) in grass-rich (green) and dicot-rich (violet) communities at Park Grass. Data points and error bars represent the mean ± SE. The dashed lines and the shaded areas represent the regression line ± CI95%. (**a**)–(**f**) adapted from Baca Cabrera *et al.* (2021a).

That no carbon fertilization effect was observed at Park Grass was also related with reductions in nitrogen acquisition during the last century, principally in the grass-rich communities (Fig. 4.2c, Table 4.1b). This matches observations in elevated CO_2 studies, which found consistently decreased rates of N acquisition in grassland, forests and crops under conditions where elevated CO_2 failed to enhance yields (Feng *et al.*, 2015). The decrease in N acquisition aggravated the N-limitation at Park Grass (all treatments were either nitrogen-limited or phosphorus- and nitrogen-co-limited), as evidenced by a significant decrease in the nitrogen nutrition index (NNI) (Lemaire *et al.*, 2008) during the last century (Table 4.1b). However, the NNI decrease was much more pronounced in grass-rich communities (−0.08, $P < 0.001$) than in dicot-rich communities (−0.04,

$P < 0.05$), and likely contributed to the negative long-term response of herbage yields in grass-rich plots.

The N acquisition long-term decreases were also negatively related to the long-term trends in $\delta^{18}O_{cellulose}$ (Fig. 4.2f), in agreement with stomatal conductance-mediated reductions of transpiration and associated mass flow-dependent N acquisition (McGrath & Lobell, 2013; Oyewole *et al.*, 2014; Feng *et al.*, 2015). The lower N acquisition reduction in the dicot-rich communities agrees with smaller reductions of stomatal conductance, but could also be associated with a stronger role of diffusion (Oyewole *et al.*, 2014) or a higher proportion of atmospheric deposition of N and biological N fixation in total N acquisition in these plots (Storkey *et al.*, 2015). Regardless of the exact mechanisms underlying the decrease in N acquisition, any impairment of N status would reduce photosynthetic capacity and feedback on stomatal conductance to adjust c_i/c_a for optimization of C gain per unit water loss by transpiration (Ainsworth & Rogers, 2007; Kattge *et al.*, 2009; Medlyn *et al.*, 2011; Smith & Keenan, 2020).

The results at Park Grass provided evidence for an interaction between plant functional groups and the c_a response of temperate-humid permanent grassland in the last century. The observed interaction was primarily associated with the much greater c_a-sensitivity of grasses in terms of their stomatal conductance compared with that of forbs and legumes, resulting in effects on grassland vegetation water-use efficiency, N acquisition and aboveground biomass production, central features of the role of vegetation in biogeochemical cycles and feedbacks to the climate system. Given that part of that evidence is correlative (but supported by empirical knowledge and mechanistic understanding obtained mostly from FACE experiments), I further explored the response mechanisms of grass leaf growth under rising c_a in the *L. perenne* experiment and discuss the key findings in the following.

4.2.2 Alterations in the diel cycle of leaf elongation of *L. perenne*

Water-use efficiency of *L. perenne* leaves increased linearly under rising c_a, at low and high VPD (Fig. 4.3a) in the mesocosms, mainly due to the large decrease in stomatal conductance and associated leaf transpiration. Differences among treatments in leaf photosynthesis were relatively small (Table 4.2). These results are also consistent with the long-term observations at Park Grass. In the same mesocosm experiment, daily mean leaf elongation rate (LER) and a suite of leaf morphogenetic parameters (leaf blade length and width, epidermal cell length) were insensitive to c_a, VPD and their interaction (Fig. 4.3b, Table 4.2), explaining, in part, the less-than expected leaf growth response towards

elevated CO_2 in FACE experiments (Ainsworth & Long, 2005). However, LER exhibited pronounced diel variation (Fig. 4.3b), with higher rates at night in all treatments ($LER_{night} > LER_{day}$, $P < 0.001$). The amplitude of the diel variation differed between treatments, due to opposite responses of leaf elongation to c_a and VPD during the day and the night. This observation pointed to different physiological mechanisms controlling leaf elongation during the night and day which resulted in a virtually-fully compensating relationship between LER_{night} and LER_{day} across all six treatments (Fig. 4.3c).

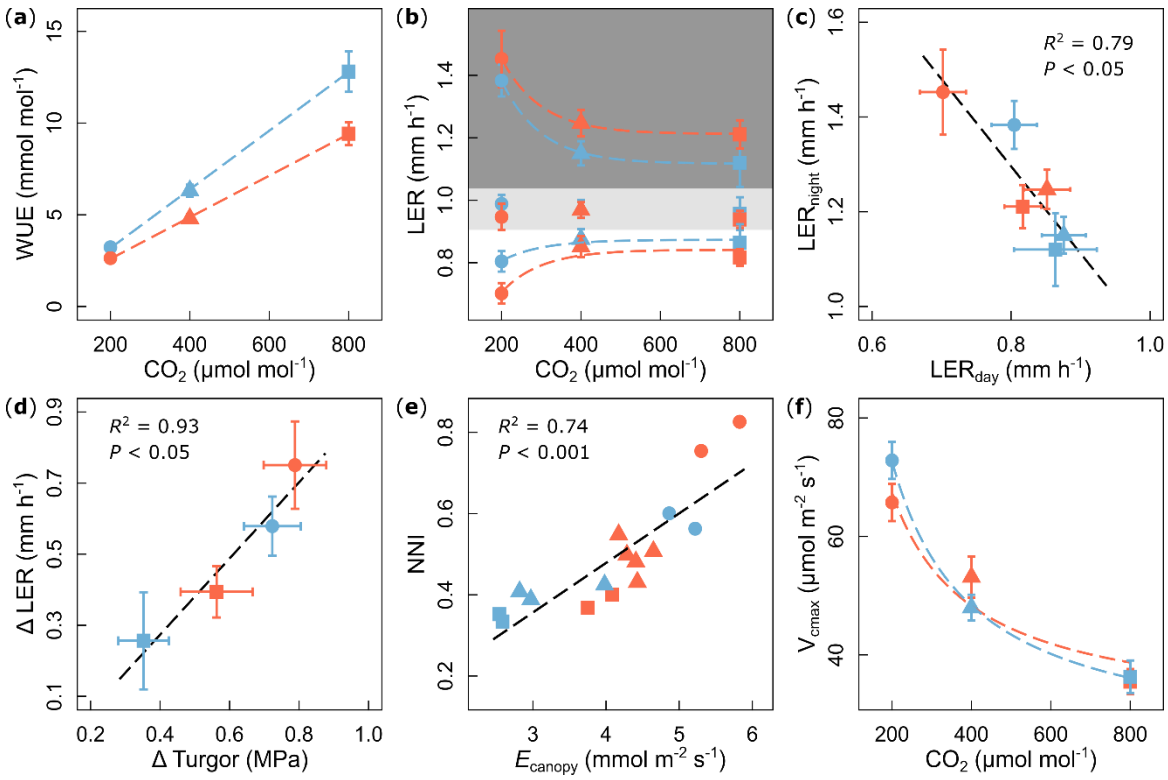

Fig. 4.3: Physiological responses of *L. perenne* to c_a and VPD. Water-use efficiency (WUE) (**a**), leaf elongation rate (LER) during the night (dark grey shaded), during the day (white background) and averaged over the entire 24 h period (light grey) (**b**), relationship between leaf elongation rate during the day (LER_{day}) and the night (LER_{night}) (**c**), and influence of the change in turgor between day and night (Δ Turgor) on the increase of LER between the day and the night period (Δ LER) of *L. perenne* leaves (**d**). Correlation between canopy transpiration (E_{canopy}) and nitrogen nutrition index (NNI) (**e**), and relationship between atmospheric CO_2 concentration and maximum rate of Rubisco carboxylation (V_{cmax}) (**f**). Symbols: circles, 200 µmol mol^{-1}; triangles, 400 µmol mol^{-1}, squares 800 µmol mol^{-1} CO_2 in the growth chamber atmosphere; blue, low VPD, red, high VPD in chamber air. Data points and error bars represent the mean ± SE. The dashed lines represent significant regression lines. NNI in (**e**) was calculated according to Lemaire *et al.* (2008). V_{cmax} in (**f**) was calculated from leaf gas exchange measurements, using the R package "Plantecophys" (Duursma, 2015). (**b**)–(**d**) adapted from Baca Cabrera *et al.* (2020).

The variation in leaf elongation during the day was controlled by a variable hydraulic limitation, resulting from the transpiration response of *L. perenne* to c_a and VPD. This was evidenced by the significant, negative effect of leaf transpiration on leaf water potential ($P < 0.05$), which resulted in a significant decrease in turgor during the day ($P < 0.01$) and LER_{day} ($P < 0.05$) with increasing leaf transpiration. Hydraulic limitation of LER_{day} occurring independently of soil water deficit has been observed repeatedly (Tardieu *et al.*, 2010; Pantin *et al.*, 2012; Caldeira *et al.*, 2014) and was related to high irradiance (Gallagher & Biscoe, 1979), high air VPD (Parrish & Wolf, 1983) or low nitrogen nutritional status (Radin & Boyer, 1982). As shown in this thesis, it can also be affected by c_a, via the alteration of stomatal conductance and transpiration.

Conversely, leaf elongation during the night showed no evidence of hydraulic limitation, as it was not significantly affected by any of the leaf hydraulic parameters assessed. Remarkably, leaf elongation during the night showed an enhancement in all treatments compared to daytime values, which fully compensated the hydraulic limitation during the day (LER averaged over a 24 h period did not differ significantly between treatments). This enhanced LER_{night} response conforms with the 'stored-growth' phenomenon that is reflected in above-normal growth when turgor recovers after a period of turgor loss and inhibited growth (Serpe & Matthews, 1994; Proseus & Boyer, 2008; Pantin *et al.*, 2012). Indeed, the enhancement of LER_{night} over LER_{day} was closely related to the nocturnal recovery of turgor (Fig. 4.3d), with the intercept of this relationship not being significantly different from 0 ($P > 0.05$).

To my knowledge, the results from the *L. perenne* experiment work demonstrated for the first time a close integration of daytime and nighttime leaf elongation in a C_3 grass under contrasting atmospheric CO_2 and VPD conditions (Baca Cabrera *et al.*, 2020). Hydraulic limitation and stored-growth caused treatment differences during the day and the night, respectively, but their balancing effects resulted in an unexpected insensitivity of leaf elongation to c_a and VPD, averaged over the entire daily cycle. Perhaps, the indirect effect of stomatal conductance on the carbon/nitrogen relationships also played a role in this mechanism. All plants received a nutrient solution with reduced N-concentration, to mimic N-limiting conditions which are common in most terrestrial ecosystems, including grasslands (LeBauer & Treseder, 2008; Terrer *et al.*, 2019). That the *L. perenne* plants were nitrogen limited was also suggested by all treatments having an epidermal cell length close to that of nitrogen-limited plants of the same cultivar of perennial ryegrass observed by Kavanová *et al.* (2008). Moreover, all treatments had a nitrogen nutrition index (NNI) < 1, with the NNI decreasing significantly with increasing c_a and VPD (Table 4.2).

NNI was closely related with canopy scale transpiration (Fig. 4.3e), indicating a reduction in the mass flow-dependent N acquisition, similar to that observed at Park Grass, which would explain the decrease in NNI with increasing c_a. Under this nitrogen limiting scenario, source limitation (White *et al.*, 2016), that is limitation by photosynthesis, appeared not to be a significant factor for leaf growth. Even at half-ambient c_a water-soluble carbohydrate concentration was greater than 53% of the dry mass of the leaf growth-and-differentiation zone in all treatments throughout the day-night cycle. Also, a very pronounced decrease in the maximum rate of Rubisco carboxylation (V_{cmax}) with c_a was evident (Fig. 4.3f); downregulation of photosynthetic capacity is a typical acclimation response at elevated CO_2, perhaps caused by an imbalance in the source/sink relationships (sink-limitation) (White *et al.*, 2016).

The *L. perenne* experiment gave insights about the feedback mechanisms between stomatal conductance and leaf growth in C_3 grasses under a changing environment. As stomatal conductance decreases under increasing c_a and VPD, the transpiration flow and the associated mass flow-dependent N acquisition may also decrease, limiting the CO_2 fertilization response. This agrees with the stomatal limitation observed at Park Grass and stresses the importance of studying the complex interactions occurring at elevated CO_2 between carbon, water and nitrogen cycles, as well as the sink-source relations, including their implication for growth processes, from the leaf to the ecosystem (Körner, 2015). It is notable that the role of stomatal conductance has been primarily investigated as a control of photosynthesis (source) or water-use efficiency, whereas its putative role in growth processes (sink) has received far less interest. It is in no way clear that understanding the latter (that is the stomatal conductance effect on growth processes) is less important to understand climate change effects on growth. Building on the present findings, studies of the diel oscillation of leaf elongation and underlying mechanism should be expanded to a greater range of plant functional groups and environmental conditions to further improve our understanding of the plant physiology of climate change adaptation.

4.3 $\delta^{18}O_{cellulose}$ as a proxy for stomatal conductance changes

In this thesis, a very pronounced decrease in stomatal conductance of grassland vegetation under rising c_a and VPD was shown, which caused a reduction in transpiration and an increase in water-use efficiency, but also had an indirect effect on nitrogen status, leaf growth processes and limitations of the carbon fertilization effect. Clearly, stomatal conductance is a central player in the regulation of various physiological processes and its response under a changing environment will strongly affect the future behavior of

grassland ecosystems. As presented here for Park Grass, reconstructive studies based on isotopic and elemental analyses of herbage samples can provide insights about the stomatal conductance responses and the associated feedbacks that already occurred in the past, and are therefore an essential complement for controlled experiments and modelling. However, there is still significant uncertainty regarding the use of $\delta^{18}O_{cellulose}$ as a proxy for stomatal conductance (Roden & Siegwolf, 2012; Gessler *et al.*, 2014). Presently, a generic quantitative model or framework linking $\delta^{18}O_{cellulose}$ to stomatal conductance is still missing.

At Park Grass, a close relationship between trends in $\delta^{18}O_{cellulose}$ and trends in the ratio of hay yield to the CO_2 concentration gradient between the atmosphere and the leaf internal gas space ($g_{s\ yield}$, another proxy of stomatal conductance integrated over the growing season and canopy, Materials and Methods) provided strong support to the idea that changes in $\delta^{18}O_{cellulose}$ are actually reflective of changes in stomatal conductance (Fig. 4.4a). Remarkably, the intercept of the regression between $\delta^{18}O_{cellulose}$ changes and $g_{s\ yield}$ change was non-significant ($P > 0.05$), suggesting that, at canopy scale, long-term changes in $\delta^{18}O_{cellulose}$, both in grass-rich and dicot-rich plots, only occurred when stomatal conductance changed. More direct approaches, such as gas exchange measurements, were not available to interpret stomatal conductance changes at Park Grass over the last century. As another alternative, the relationship between $\delta^{18}O_{cellulose}$ and stomatal conductance was also investigated using the process-based model MuSICA, parameterized for the Grünschwaige temperate humid grassland for the 2006–2012 period (Hirl *et al.*, 2019; Hirl *et al.*, 2021). In that study, $\Delta^{18}O$ of leaf cellulose samples ($\Delta^{18}O_{cellulose}$) decreased significantly with increasing midday canopy-scale stomatal conductance (Fig. 4.4b), as is expected from theoretical (although qualitative) considerations and observations reported elsewhere (see Table S2 in Baca Cabrera *et al.*, 2021a for a list of publications). These lines of evidence also supported the interpretation that the long-term $\delta^{18}O_{cellulose}$ increase observed at Park Grass was associated with a long-term decrease in stomatal conductance.

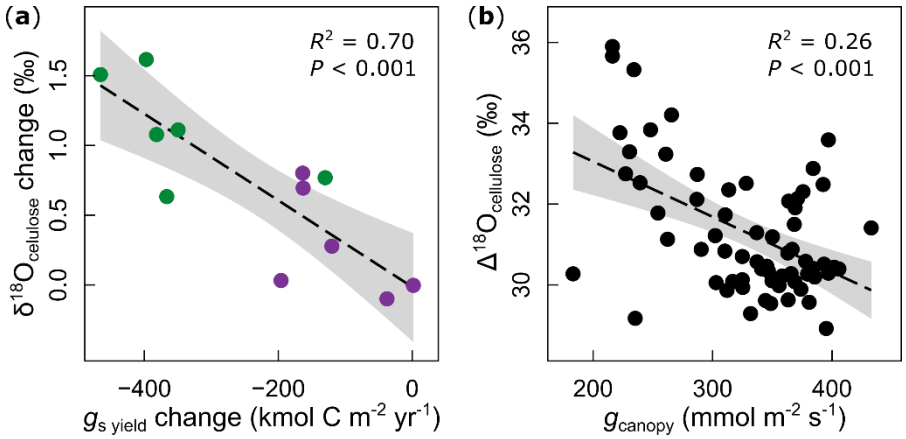

Fig. 4.4: Relationship between stomatal conductance and $\delta^{18}O_{cellulose}$. Relationship between long-term changes in canopy-scale, growing season-integrated stomatal conductance ($g_{s\ yield}$) and $\delta^{18}O_{cellulose}$ in grass-rich (green) and dicot-rich (violet) communities at Park Grass (**a**) (adapted from Baca Cabrera *et al.*, 2021a); and relationship between midday canopy-scale stomatal conductance (g_{canopy}) and $\Delta^{18}O_{cellulose}$, averaged over the integration time (the maximum age of structural leaf biomass in a sample) at the Grünschwaige temperate humid grassland (**b**) (adapted from Hirl *et al.*, 2021). Data points represent treatment means in (**a**) and individual measurements in (**b**). The dashed lines and the shaded areas represent the regression line ± CI95%.

Nevertheless, the large scatter in the relationship between $\delta^{18}O_{cellulose}$ (or $\Delta^{18}O_{cellulose}$) and stomatal conductance in the MuSICA simulations as well as among the empirical studies reported elsewhere (Baca Cabrera *et al.*, 2021a), demonstrate that there is no simple, reliable empirical relationship between $\delta^{18}O_{cellulose}$ (or $\Delta^{18}O_{cellulose}$) changes and stomatal conductance changes. Clearly, these realizations points to the need for a better mechanistic understanding of the relationship between $\delta^{18}O_{cellulose}$ and stomatal conductance. Accordingly, the last part of my dissertation was devoted to the study of two specific details of that relationship, namely (1) the role of photosynthetic and post-photosynthetic factors in shaping the $\delta^{18}O_{cellulose}$ signal in *L. perenne* exposed to contrasting atmospheric CO_2 and VPD levels, and (2) the assumption that $\Delta^{18}O_{SucSynW}$ is equal to $\Delta^{18}O_{LW}$ in the Barbour & Farquhar (2000) model that relates $\Delta^{18}O_{Cellulose}$ to ^{18}O-enrichment of water in photosynthesizing leaves (Baca Cabrera *et al.*, 2021b).

In principle, $\delta^{18}O_{Cellulose}$ results from the isotopic mixing of two water pools: (1) leaf water, which becomes evaporatively enriched in ^{18}O during transpiration, and imprints its isotopic signal onto the $\delta^{18}O$ of photosynthetic products, including sucrose (that is a 'photosynthetic signal' derived from sucrose synthesis water) and (2) unenriched water at the site of cellulose synthesis, which exchanges oxygen with the metabolic intermediates of cellulose synthesis, thus attenuating the original photosynthetic $\delta^{18}O$ signal during 'post-photosynthesis' processes (cf. Eqn 1.3). (1) is principally sensitive to stomatal

conductance, but responds especially strongly to atmospheric humidity (Cernusak *et al.*, 2016). The proportional contributions (as fractions of 1) of sucrose synthesis water and unenriched water to ^{18}O-enrichment of cellulose above source water ($\Delta^{18}O_{Cellulose}$) are given by the terms ($1 - p_{ex}p_x$) and $p_{ex}p_x$ in Eqn 1.3. Although the term $p_{ex}p_x$ cannot be measured directly, it can be estimated by solving Eqn 1.3, if the $\Delta^{18}O_{Cellulose}$ and $\Delta^{18}O_{SucSynW}$ are known.

The results of this study clearly showed a discrepancy between $\Delta^{18}O_{LW}$ and $\Delta^{18}O_{SucSynW}$, when the latter was estimated as the difference between $\Delta^{18}O_{sucrose}$ and the temperature dependent ε_{bio} observed by Sternberg & Ellsworth (2011) (26.7‰ at 20°C, the air temperature in the growth chambers). A similar deviation had already been noted by Lehmann *et al.* (2017). $\Delta^{18}O_{SucSynW}$ was more enriched than $\Delta^{18}O_{LW}$ in all treatments, with the difference being much more pronounced at high than at low VPD (+8.5‰ vs. +2.2‰; $P < 0.001$), which contradicts the common assumption of previous works that $\Delta^{18}O_{SucSynW}$ equals $\Delta^{18}O_{LW}$ (Barbour, 2007). The fact that $\Delta^{18}O_{SucSynW}$ was significantly higher than $\Delta^{18}O_{LW}$ must have resulted from photosynthesis and associated sucrose synthesis being closer to the evaporative sites and/or situated in the distal half of the leaf blades, where ^{18}O-enrichment of leaf water is much greater (Helliker & Ehleringer, 2000; Helliker & Ehleringer, 2002; Gan *et al.*, 2003; Affek *et al.*, 2006; Ogée *et al.*, 2007). That effect was not influenced by CO_2 ($P > 0.05$, Table 4.2) and appeared to be stable throughout diurnal cycles, as $\Delta^{18}O_{Sucrose}$ across treatments was very similar at the end of the day (41.5‰) and the end of the night (40.9‰) (Table 4.2).

The isotopic discrepancy between $\Delta^{18}O_{LW}$ and $\Delta^{18}O_{SucSynW}$ had major implications for the interpretation of the ^{18}O signal transfer and its attribution to photosynthetic and post-photosynthetic factors within the Barbour & Farquhar (2000) model given by Eqn 1.3. When related to $\Delta^{18}O_{SucSynW}$ the model predicted a virtually constant $p_{ex}p_x$ (termed $p_{ex}p_{x\text{-}SucSynW}$) of ~0.50 (±0.02 SE) across environmental conditions, indicating that post-photosynthetically exchanged oxygen in cellulose was a constant fraction, and hence environmentally-driven variation of $\Delta^{18}O_{Cellulose}$ reflected purely a photosynthetic signal. Conversely, when interpreted with respect to $\Delta^{18}O_{LW}$, $p_{ex}p_x$ (termed $p_{ex}p_{x\text{-}LW}$) varied strongly, particularly as a function of VPD (or air relative humidity, RH, as temperature was the same in all chambers). That variation of $p_{ex}p_{x\text{-}LW}$ must be recognized as an artifact, resulting from the failure of $\Delta^{18}O_{LW}$ to predict accurately $\Delta^{18}O_{SucSynW}$. That RH-dependent artifact on $p_{ex}p_{x\text{-}LW}$ wrongly suggested an RH-dependent variation of post-photosynthetic oxygen exchange during metabolic processes connected with oxygen incorporation in cellulose. These results also explain why Hirl *et al.* (2021) had to use a RH-sensitive $p_{ex}p_x$

when predicting $\Delta^{18}O_{Cellulose}$ from modelling of $\Delta^{18}O_{LW}$ in the Grünschwaige grassland. In that, this observation also indicates strongly that the mechanism observed in controlled environments also occurs in natural conditions.

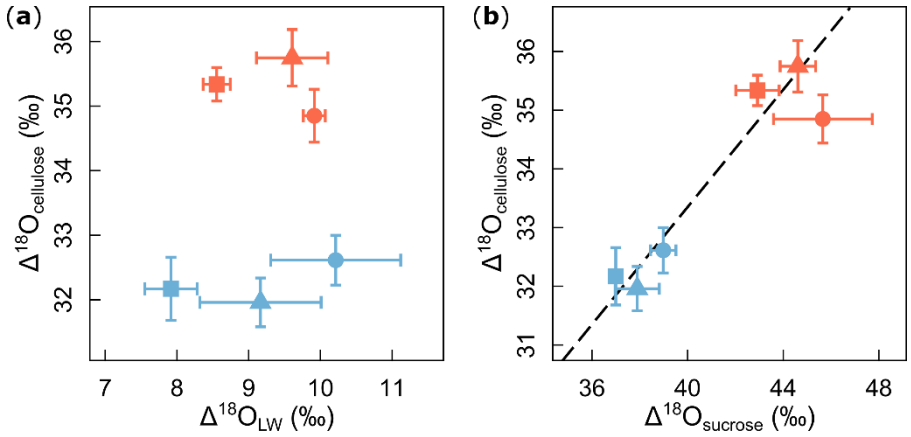

Fig. 4.5: ^{18}O-enrichment of leaf water, leaf sucrose and leaf cellulose in *L. perenne*. Relationship between $\Delta^{18}O$ of bulk leaf water ($\Delta^{18}O_{LW}$) and $\Delta^{18}O$ of cellulose ($\Delta^{18}O_{cellulose}$) (**a**) and between $\Delta^{18}O$ of sucrose ($\Delta^{18}O_{sucrose}$) and $\Delta^{18}O_{cellulose}$ (**b**) in *L. perenne* leaves as affected by atmospheric CO_2 concentration (circles, 200 µmol mol^{-1}; triangles, 400 µmol mol^{-1}; squares, 800 µmol mol^{-1}) and vapor pressure deficit (VPD) (low VPD, blue; high VPD, red) in the mesocosm experiment. Data points and error bars represent the mean ± SE. The dashed line in (**b**) indicates the $\Delta^{18}O_{cellulose}$ values predicted with the Barbour–Farquhar model with $p_{ex}p_x$ = 0.5 and ε_{bio} at 20°C (26.7‰). (**a**) and (**b**) adapted from Baca Cabrera *et al.* (2021b).

The results presented here demonstrated for the first time the constancy of $p_{ex}p_{x\text{-}SucSynW}$ across c_a and VPD gradients in a model C_3 grass, a finding of central importance for the interpretation of long-term reconstructive studies of $\delta^{18}O_{cellulose}$ in terms of stomatal conductance changes in grassland vegetation. That constancy supports the idea that long-term changes in $\Delta^{18}O_{cellulose}$ actually reflect a photosynthetic signal, rather than post-photosynthetic processes.

4.4 Conclusions and perspectives

The present work indicated a strong sensitivity of stomatal conductance to c_a, vapor pressure deficit and their interaction in grassland vegetation. This was evidenced both by the consistent decrease in stomatal conductance during the last century at Park Grass and by the pronounced response of *L. perenne* to atmospheric CO_2 (and VPD) in controlled environment experiments. Stomatal conductance changes affected plant transpiration, water-use efficiency, N acquisition and aboveground biomass production, central features of the role of vegetation in biogeochemical cycles and feedbacks to the climate system. Stomatal control does not only determine the tradeoff between carbon gain and water loss

under changing environmental conditions, but can ultimately affect integrating plant processes such as leaf growth and its diurnal oscillation, as demonstrated in the *L. perenne* experiment.

This thesis also showed that key predictions drawn from FACE experiments regarding limitations of the carbon fertilization effect (Lüscher *et al.*, 2004; Ainsworth & Long, 2005; Körner, 2006), reductions in N acquisition (Feng *et al.*, 2015) and a greater stomatal limitation of the CO_2 response in grasses relative to forbs and legumes (Lüscher *et al.*, 2004; Ainsworth & Rogers, 2007) have already taken hold in some temperate grasslands under N-limiting conditions in the last century or before. This highlights the importance of reconstructive studies for a better understanding of the stomatal conductance response of grassland vegetation in a changing environment.

Finally, on the basis of the findings of this work, the following research topics should be addressed in detail in future investigations. First, the results presented here and also observed in FACE experiments (Ainsworth & Rogers, 2007) showed a pronounced negative response of stomatal conductance of grasses to c_a and a resulting limitation of photosynthesis. However, mesophyll conductance, the conductance between the intercellular air spaces and the site of carboxylation, also significantly constrains the rate of photosynthesis (Flexas *et al.*, 2012; Tholen *et al.*, 2012). Most gas exchange studies (including the leaf gas exchange measurements presented here) assume mesophyll conductance to be large and constant, a simplification that may be unrealistic (Flexas *et al.*, 2012). However, mesophyll conductance is actually tightly coupled with stomatal conductance (Flexas *et al.*, 2013; Dewar *et al.*, 2018; Ma *et al.*, 2021) and a significant negative response of mesophyll conductance to CO_2 has been reported (Flexas *et al.*, 2012). Thus, future studies of photosynthetic limitations under rising c_a should investigate both stomatal and mesophyll conductance responses, especially considering that the acclimation response of the latter is still uncertain (Flexas *et al.*, 2012). Second, future experiments regarding the effects of global change in grassland vegetation should look more closely into the direct role of stomatal (and mesophyll) conductance as a control of photosynthesis (source limitation), but also its putative role in the growth processes (sink), a topic that has received far less attention. As discussed in detail elsewhere, such an approach requires a “paradigm shift” (Körner, 2015; Körner, 2021) from a carbon centric view to more integrating analyses that explore the complex relationships and feedbacks between carbon, water and nutrients in plants under a changing environment. And, third, considering that $\delta^{18}O_{cellulose}$ reconstructive studies are a precious tool for understanding the adaptation of grassland vegetation to climate change, further efforts should explore in

greater detail the mechanisms connecting stomatal conductance and $\delta^{18}O_{cellulose}$. This will likely involve studies of the spatio-temporal dynamics of ^{18}O-enrichment within leaves – from base to tip, from center to margin and from vascular tissue to evaporative sites – and the parallel patterns of photosynthesis and associated sucrose synthesis.

References

Affek HP, Krisch MJ, Yakir D. 2006. Effects of intraleaf variations in carbonic anhydrase activity and gas exchange on leaf $C^{18}OO$ isoflux in *Zea mays*. *New Phytologist* **169**: 321-329.

Ainsworth EA, Long SP. 2005. What have we learned from 15 years of free-air CO_2 enrichment (FACE)? A meta-analytic review of the responses of photosynthesis, canopy properties and plant production to rising CO_2. *New Phytologist* **165**: 351-372.

Ainsworth EA, Rogers A. 2007. The response of photosynthesis and stomatal conductance to rising [CO_2]: mechanisms and environmental interactions. *Plant, Cell & Environment* **30**: 258-270.

Arneth A, Harrison SP, Zaehle S, Tsigaridis K, Menon S, Bartlein PJ, Feichter J, Korhola A, Kulmala M, O'Donnell D, *et al*. 2010. Terrestrial biogeochemical feedbacks in the climate system. *Nature Geoscience* **3**: 525-532.

Baca Cabrera JC, Hirl RT, Schäufele R, Macdonald A, Schnyder H. 2021a. Stomatal conductance limited the CO_2 response of grassland in the last century. *BMC Biology* **19**: 50. doi: 10.1186/s12915-021-00988-4.

Baca Cabrera JC, Hirl RT, Schäufele R, Zhu J, Liu HT, Ogée J, Schnyder H. 2021b. ^{18}O enrichment of leaf cellulose correlated with ^{18}O enrichment of leaf sucrose but not bulk leaf water in a C_3 grass across contrasts of atmospheric CO_2 concentration and air humidity. *Research Square*. doi: 10.21203/rs.3.rs-596094/v1.

Baca Cabrera JC, Hirl RT, Zhu J, Schäufele R, Schnyder H. 2020. Atmospheric CO_2 and VPD alter the diel oscillation of leaf elongation in perennial ryegrass: compensation of hydraulic limitation by stored-growth. *New Phytologist* **227**: 1776-1789.

Barbosa ICR, Köhler IH, Auerswald K, Lüps P, Schnyder H. 2010. Last-century changes of alpine grassland water-use efficiency: a reconstruction through carbon isotope analysis of a time-series of *Capra ibex* horns. *Global Change Biology* **16**: 1171-1180.

Barbour MM. 2007. Stable oxygen isotope composition of plant tissue: a review. *Functional Plant Biology* **34**: 83-94.

Barbour MM, Farquhar GD. 2000. Relative humidity- and ABA-induced variation in carbon and oxygen isotope ratios of cotton leaves. *Plant, Cell & Environment* **23**: 473-485.

Barbour MM, Fischer RA, Sayre KD, Farquhar GD. 2000. Oxygen isotope ratio of leaf and grain material correlates with stomatal conductance and grain yield in irrigated wheat. *Functional Plant Biology* **27**: 625-637.

Barnard HR, Brooks JR, Bond BJ. 2012. Applying the dual-isotope conceptual model to interpret physiological trends under uncontrolled conditions. *Tree Physiology* **32**: 1183-1198.

Bernacchi CJ, VanLoocke A. 2015. Terrestrial ecosystems in a changing environment: a dominant role for water. *Annual Review of Plant Biology* **66**: 599-622.

Berry JA, Beerling DJ, Franks PJ. 2010. Stomata: key players in the earth system, past and present. *Current Opinion in Plant Biology* **13**: 232-239.

Bowes G. 1993. Facing the inevitable: plants and increasing atmospheric CO_2. *Annual Review of Plant Physiology and Plant Molecular Biology* **44**: 309-332.

Brendel O, Iannetta PPM, Stewart D. 2000. A rapid and simple method to isolate pure alpha-cellulose. *Phytochemical Analysis* **11**: 7-10.

Buckley TN. 2017. Modeling stomatal conductance. *Plant Physiology* **174**: 572-582.

Buckley TN, Schymanski SJ. 2014. Stomatal optimisation in relation to atmospheric CO_2. *New Phytologist* **201**: 372-377.

Caldeira CF, Bosio M, Parent B, Jeanguenin L, Chaumont F, Tardieu F. 2014. A hydraulic model is compatible with rapid changes in leaf elongation rate under fluctuating evaporative demand and soil water status. *Plant Physiology* **164**: 1718-1730.

Campbell JE, Berry JA, Seibt U, Smith SJ, Montzka SA, Launois T, Belviso S, Bopp L, Laine M. 2017. Large historical growth in global terrestrial gross primary production. *Nature* **544**: 84-87.

Cernusak LA, Barbour MM, Arndt SK, Cheesman AW, English NB, Feild TS, Helliker BR, Holloway-Phillips MM, Holtum JAM, Kahmen A, *et al*. 2016. Stable isotopes in leaf water of terrestrial plants. *Plant, Cell & Environment* **39**: 1087-1102.

Cernusak LA, Farquhar GD, Pate JS. 2005. Environmental and physiological controls over oxygen and carbon isotope composition of Tasmanian blue gum, *Eucalyptus globulus*. *Tree Physiology* **25**: 129-146.

Cernusak LA, Ubierna N, Winter K, Holtum JAM, Marshall JD, Farquhar GD. 2013. Environmental and physiological determinants of carbon isotope discrimination in terrestrial plants. *New Phytologist* **200**: 950-965.

Cernusak LA, Wong SC, Farquhar GD. 2003. Oxygen isotope composition of phloem sap in relation to leaf water in *Ricinus communis*. *Functional Plant Biology* **30**: 1059-1070.

Craine JM, Elmore AJ, Wang L, Aranibar J, Bauters M, Boeckx P, Crowley BE, Dawes MA, Delzon S, Fajardo A, *et al*. 2018. Isotopic evidence for oligotrophication of terrestrial ecosystems. *Nature Ecology & Evolution* **2**: 1735-1744.

Dawson TE, Mambelli S, Plamboeck AH, Templer PH, Tu KP. 2002. Stable isotopes in plant ecology. *Annual Review of Ecology and Systematics* **33**: 507-559.

DeNiro MJ, Epstein S. 1979. Relationship between the oxygen isotope ratios of terrestrial plant cellulose, carbon dioxide, and water. *Science* **204**: 51-53.

Dewar R, Mauranen A, Mäkelä A, Hölttä T, Medlyn B, Vesala T. 2018. New insights into the covariation of stomatal, mesophyll and hydraulic conductances from optimization models incorporating nonstomatal limitations to photosynthesis. *New Phytologist* **217**: 571-585.

Dixon AP, Faber-Langendoen D, Josse C, Morrison J, Loucks CJ. 2014. Distribution mapping of world grassland types. *Journal of Biogeography* **41**: 2003-2019.

Dlugokencky EJ, Mund JW, Crotwell AM, Crotwell MJ, Thoning KW 2019. Atmospheric carbon dioxide dry air mole fractions from the NOAA ESRL carbon cycle cooperative global air sampling network, 1968-2018. https://doi.org/10.15138/wkgj-f215.

Dodd ME, Silvertown J, McConway K, Potts J, Crawley M. 1994. Stability in the plant communities of the Park Grass Experiment: the relationships between species richness, soil pH and biomass variability. *Philosophical Transactions of the Royal Society of London. Series B: Biological Sciences* **346**: 185-193.

Drake BG, Gonzàlez-Meler MA, Long SP. 1997. More efficient plants: a consequence of rising atmospheric CO_2? *Annual Review of Plant Physiology and Plant Molecular Biology* **48**: 609-639.

Du E, Terrer C, Pellegrini AFA, Ahlström A, van Lissa CJ, Zhao X, Xia N, Wu X, Jackson RB. 2020. Global patterns of terrestrial nitrogen and phosphorus limitation. *Nature Geoscience* **13**: 221-226.

Dusenge ME, Duarte AG, Way DA. 2019. Plant carbon metabolism and climate change: elevated CO_2 and temperature impacts on photosynthesis, photorespiration and respiration. *New Phytologist* **221**: 32-49.

Duursma RA. 2015. Plantecophys - an R package for analysing and modelling leaf gas exchange data. *PLoS ONE* **10**: e0143346.

Ehleringer JR, Hall AE, Farquhar GD. 1993. *Stable isotopes and plant carbon-water relations*. San Diego: Academic Press

Farquhar GD, Barbour MM, Henry BK 1998. Interpretation of oxygen isotope composition of leaf material. In: Griffiths H, ed. *Stable isotopes: integration of biological, ecological and geochemical processes*. Oxford, UK: BIOS Scientific Publishers, 27-61.

Farquhar GD, Ehleringer JR, Hubick KT. 1989. Carbon isotope discrimination and photosynthesis. *Annual Review of Plant Biology* **40**: 503-537.

Farquhar GD, O'Leary MH, Berry JA. 1982. On the relationship between carbon isotope discrimination and the intercellular carbon dioxide concentration in leaves. *Australian Journal of Plant Physiology* **9**: 121-137.

Farquhar GD, Richards RA. 1984. Isotopic composition of plant carbon correlates with water-use efficiency ofwheat genotypes. *Australian Journal of Plant Physiology* **11**: 539-552.

Feng Z, Rütting T, Pleijel H, Wallin G, Reich PB, Kammann CI, Newton PCD, Kobayashi K, Luo Y, Uddling J. 2015. Constraints to nitrogen acquisition of terrestrial plants under elevated CO_2. *Global Change Biology* **21**: 3152-3168.

Ferris R, Nijs I, Behaeghe T, Impens I. 1996. Contrasting CO_2 and temperature effects on leaf growth of perennial ryegrass in spring and summer. *Journal of Experimental Botany* **47**: 1033-1043.

Field CB, Lobell DB, Peters HA, Chiariello NR. 2007. Feedbacks of terrestrial ecosystems to climate change. *Annual Review of Environment and Resources* **32**: 1-29.

Flexas J, Barbour MM, Brendel O, Cabrera HM, Carriquí M, Diaz-Espejo A, Douthe C, Dreyer E, Ferrio JP, Gago J, *et al*. 2012. Mesophyll diffusion conductance to CO_2: an unappreciated central player in photosynthesis. *Plant Science* **193-194**: 70-84.

Flexas J, Niinemets Ü, Gallé A, Barbour MM, Centritto M, Diaz-Espejo A, Douthe C, Galmés J, Ribas-Carbo M, Rodriguez PL, *et al*. 2013. Diffusional conductances to CO_2 as a target for increasing photosynthesis and photosynthetic water-use efficiency. *Photosynthesis Research* **117**: 45-59.

Foley JA, Ramankutty N, Brauman KA, Cassidy ES, Gerber JS, Johnston M, Mueller ND, O'Connell C, Ray DK, West PC, *et al*. 2011. Solutions for a cultivated planet. *Nature* **478**: 337-342.

Franks PJ, Adams MA, Amthor JS, Barbour MM, Berry JA, Ellsworth DS, Farquhar GD, Ghannoum O, Lloyd J, McDowell N, et al. 2013. Sensitivity of plants to changing atmospheric CO2 concentration: from the geological past to the next century. *New Phytologist* **197**: 1077-1094.

Franks PJ, Farquhar GD. 2007. The mechanical diversity of stomata and its significance in gas-exchange control. *Plant Physiology* **143**: 78-87.

Friedli H, Lötscher H, Oeschger H, Siegenthaler U, Stauffer B. 1986. Ice core record of the $^{13}C/^{12}C$ ratio of atmospheric CO_2 in the past two centuries. *Nature* **324**: 237-238.

Friedlingstein P, Meinshausen M, Arora VK, Jones CD, Anav A, Liddicoat SK, Knutti R. 2014. Uncertainties in CMIP5 climate projections due to carbon cycle feedbacks. *Journal of Climate* **27**: 511-526.

Friend AD, Arneth A, Kiang NY, Lomas M, Ogée J, Rödenbeck C, Running SW, Santaren J-D, Sitch S, Viovy N, *et al*. 2007. FLUXNET and modelling the global carbon cycle. *Global Change Biology* **13**: 610-633.

Gallagher JN, Biscoe PV. 1979. Field studies of cereal leaf growth: III. Barley leaf extension in relation to temperature, irradiance and water potential. *Journal of Experimental Botany* **30**: 645-655.

Gan KS, Wong SC, Yong JWH, Farquhar GD. 2003. Evaluation of models of leaf water ^{18}O enrichment using measurements of spatial patterns of vein xylem water, leaf water and dry matter in maize leaves. *Plant, Cell & Environment* **26**: 1479-1495.

Gaudinski JB, Dawson TE, Quideau S, Schuur EAG, Roden JS, Trumbore SE, Sandquist DR, Oh S-W, Wasylishen RE. 2005. Comparative analysis of cellulose preparation techniques for use with ^{13}C, ^{14}C, and ^{18}O isotopic measurements. *Analytical Chemistry* **77**: 7212-7224.

Gebbing T, Schnyder H. 2001. ^{13}C Labeling kinetics of sucrose in glumes indicates significant refixation of respiratory CO_2 in the wheat ear. *Functional Plant Biology* **28**: 1047-1053.

Gentine P, Green JK, Guérin M, Humphrey V, Seneviratne SI, Zhang Y, Zhou S. 2019. Coupling between the terrestrial carbon and water cycles—a review. *Environmental Research Letters* **14**: 083003.

Gessler A, Ferrio JP, Hommel R, Treydte K, Werner RA, Monson RK. 2014. Stable isotopes in tree rings: towards a mechanistic understanding of isotope fractionation and mixing processes from the leaves to the wood. *Tree Physiology* **34**: 796-818.

Giuggiola A, Ogée J, Rigling A, Gessler A, Bugmann H, Treydte K. 2016. Improvement of water and light availability after thinning at a xeric site: which matters more? A dual isotope approach. *New Phytologist* **210**: 108-121.

Grams TEE, Kozovits AR, Häberle K-H, Matyssek R, Dawson TE. 2007. Combining $\delta^{13}C$ and $\delta^{18}O$ analyses to unravel competition, CO_2 and O_3 effects on the physiological performance of different-aged trees. *Plant, Cell & Environment* **30**: 1023-1034.

Grossiord C, Buckley TN, Cernusak LA, Novick KA, Poulter B, Siegwolf RTW, Sperry JS, McDowell NG. 2020. Plant responses to rising vapor pressure deficit. *New Phytologist* **226**: 1550-1566.

Guerrieri R, Belmecheri S, Ollinger SV, Asbjornsen H, Jennings K, Xiao J, Stocker BD, Martin M, Hollinger DY, Bracho-Garrillo R, *et al*. 2019. Disentangling the role of photosynthesis and stomatal conductance on rising forest water-use efficiency. *Proceedings of the National Academy of Sciences* **116**: 16909-16914.

Helliker BR, Ehleringer JR. 2000. Establishing a grassland signature in veins: ^{18}O in the leaf water of C_3 and C_4 grasses. *Proceedings of the National Academy of Science* **97**: 7894-7898.

Helliker BR, Ehleringer JR. 2002. Grass blades as tree rings: environmentally induced changes in the oxygen isotope ratio of cellulose along the length of grass blades. *New Phytologist* **155**: 417-424.

Hetherington AM, Woodward FI. 2003. The role of stomata in sensing and driving environmental change. *Nature* **424**: 901-908.

Hirl RT, Ogée J, Ostler U, Schäufele R, Baca Cabrera JC, Zhu J, Schleip I, Wingate L, Schnyder H. 2021. Temperature-sensitive biochemical ^{18}O-fractionation and humidity-dependent attenuation factor are needed to predict $\delta^{18}O$ of cellulose from leaf water in a grassland ecosystem. *New Phytologist* **229**: 3156-3171.

Hirl RT, Schnyder H, Ostler U, Schäufele R, Schleip I, Vetter SH, Auerswald K, Baca Cabrera JC, Wingate L, Barbour MM, *et al*. 2019. The ^{18}O ecohydrology of a grassland ecosystem – predictions and observations. *Hydrol. Earth Syst. Sci.* **23**: 2581-2600.

Hovenden MJ, Leuzinger S, Newton PCD, Fletcher A, Fatichi S, Lüscher A, Reich PB, Andresen LC, Beier C, Blumenthal DM, *et al*. 2019. Globally consistent

influences of seasonal precipitation limit grassland biomass response to elevated CO_2. *Nature Plants* **5**: 167-173.

Jenkinson DS, Potts JM, Perry JN, Barnett V, Coleman K, Johnston AE. 1994. Trends in herbage yields over the last century on the Rothamsted Long-term Continuous Hay Experiment. *The Journal of Agricultural Science* **122**: 365-374.

Kattge J, Knorr W, Raddatz T, Wirth C. 2009. Quantifying photosynthetic capacity and its relationship to leaf nitrogen content for global-scale terrestrial biosphere models. *Global Change Biology* **15**: 976-991.

Katul GG, Manzoni S, Palmroth S, Oren R. 2010. A stomatal optimization theory to describe the effects of atmospheric CO2 on leaf photosynthesis and transpiration. *Annals of Botany* **105**: 431-442.

Katul GG, Palmroth S, Oren R. 2009. Leaf stomatal responses to vapour pressure deficit under current and CO_2-enriched atmosphere explained by the economics of gas exchange. *Plant, Cell & Environment* **32**: 968-979.

Kavanová M, Lattanzi FA, Schnyder H. 2008. Nitrogen deficiency inhibits leaf blade growth in *Lolium perenne* by increasing cell cycle duration and decreasing mitotic and post-mitotic growth rates. *Plant, Cell & Environment* **31**: 727-737.

Keenan TF, Williams CA. 2018. The terrestrial carbon sink. *Annual Review of Environment and Resources* **43**: 219-243.

Kimball BA. 2016. Crop responses to elevated CO_2 and interactions with H_2O, N, and temperature. *Current Opinion in Plant Biology* **31**: 36-43.

Köhler IH, Poulton PR, Auerswald K, Schnyder H. 2010. Intrinsic water-use efficiency of temperate seminatural grassland has increased since 1857: an analysis of carbon isotope discrimination of herbage from the Park Grass Experiment. *Global Change Biology* **16**: 1531-1541.

Körner C. 2006. Plant CO_2 responses: an issue of definition, time and resource supply. *New Phytologist* **172**: 393-411.

Körner C. 2015. Paradigm shift in plant growth control. *Current Opinion in Plant Biology* **25**: 107-114.

Körner C 2021. Tools Shape Paradigms of Plant-Environment Interactions. In: Cánovas FM, Lüttge U, Risueño M-C, Pretzsch H, eds. *Progress in Botany, vol. 82*. Cham: Springer, 1-41.

Leakey ADB, Ainsworth EA, Bernacchi CJ, Rogers A, Long SP , Ort DR. 2009. Elevated CO_2 effects on plant carbon, nitrogen, and water relations: six important lessons from FACE. *Journal of Experimental Botany* **60**: 2859-2876.

Leakey ADB, Ferguson JN, Pignon CP, Wu A, Jin Z, Hammer GL, Lobell DB. 2019. Water use efficiency as a constraint and target for improving the resilience and productivity of C_3 and C_4 crops. *Annual Review of Plant Biology* **70**: 781-808.

LeBauer DS, Treseder KK. 2008. Nitrogen limitation of net primary productivity in terrestrial ecosystems is globally distributed. *Ecology* **89**: 371-379.

Lehmann MM, Gamarra B, Kahmen A, Siegwolf RT, Saurer M. 2017. Oxygen isotope fractionations across individual leaf carbohydrates in grass and tree species. *Plant, Cell & Environment* **40**: 1658-1670.

Lehmeier CA, Lattanzi FA, Schäufele R, Wild M, Schnyder H. 2008. Root and shoot respiration of perennial ryegrass are supplied by the same substrate pools: assessment by dynamic ^{13}C labeling and compartmental analysis of tracer kinetics. *Plant Physiology* **148**: 1148-1158.

Lemaire G, Jeuffroy M-H, Gastal F. 2008. Diagnosis tool for plant and crop N status in vegetative stage: Theory and practices for crop N management. *European Journal of Agronomy* **28**: 614-624.

Liu HT, Gong XY, Schäufele R, Yang F, Hirl RT, Schmidt A, Schnyder H. 2016. Nitrogen fertilization and $\delta^{18}O$ of CO_2 have no effect on ^{18}O-enrichment of leaf water and cellulose in *Cleistogenes squarrosa* (C_4) – is VPD the sole control? *Plant, Cell & Environment* **39**: 2701-2712.

Liu HT, Schäufele R, Gong XY, Schnyder H. 2017. The $\delta^{18}O$ and $\delta^{2}H$ of water in the leaf growth-and-differentiation zone of grasses is close to source water in both humid and dry atmospheres. *New Phytologist* **214**: 1423-1431.

Lüscher A, Daepp M, Blum H, Hartwig UA, Nösberger J. 2004. Fertile temperate grassland under elevated atmospheric CO_2—role of feed-back mechanisms and availability of growth resources. *European Journal of Agronomy* **21**: 379-398.

Ma WT, Tcherkez G, Wang XM, Schäufele R, Schnyder H, Yang Y, Gong XY. 2021. Accounting for mesophyll conductance substantially improves ^{13}C-based estimates of intrinsic water-use efficiency. *New Phytologist* **229**: 1326-1338.

Macdonald A, Poulton P, Clark I, Scott T, Glendining M, Perryman S, Storkey J, Bell J, Shield I, McMillan V, *et al*. 2018. Rothamsted Long-term experiments : guide to the classical and other long-term experiments, datasets and sample archive. Harpenden, UK: Rothamsted Research.

Masle J. 2000. The effects of elevated CO_2 concentrations on cell division rates, growth patterns, and blade anatomy in young wheat plants are modulated by factors related to leaf position, vernalization, and genotype. *Plant Physiology* **122**: 1399-1415.

McAdam SAM, Brodribb TJ. 2015. The evolution of mechanisms driving the stomatal response to vapor pressure deficit. *Plant Physiology* **167**: 833-843.

McGrath JM, Lobell DB. 2013. Reduction of transpiration and altered nutrient allocation contribute to nutrient decline of crops grown in elevated CO_2 concentrations. *Plant, Cell & Environment* **36**: 697-705.

Medlyn BE, De Kauwe MG, Lin Y-S, Knauer J, Duursma RA, Williams CA, Arneth A, Clement R, Isaac P, Limousin J-M, *et al*. 2017. How do leaf and ecosystem measures of water-use efficiency compare? *New Phytologist* **216**: 758-770.

Medlyn BE, Duursma RA, De Kauwe MG, Prentice IC. 2013. The optimal stomatal response to atmospheric CO_2 concentration: Alternative solutions, alternative interpretations. *Agricultural and Forest Meteorology* **182-183**: 200-203.

Medlyn BE, Duursma RA, Eamus D, Ellsworth DS, Prentice IC, Barton CVM, Crous KY, De Angelis P, Freeman M, Wingate L. 2011. Reconciling the optimal and empirical approaches to modelling stomatal conductance. *Global Change Biology* **17**: 2134-2144.

Moreno-Gutiérrez C, Dawson TE, Nicolás E, Querejeta JI. 2012. Isotopes reveal contrasting water use strategies among coexisting plant species in a Mediterranean ecosystem. *New Phytologist* **196**: 489-496.

Nowak RS, Ellsworth DS, Smith SD. 2004. Functional responses of plants to elevated atmospheric CO_2 – do photosynthetic and productivity data from FACE experiments support early predictions? *New Phytologist* **162**: 253-280.

Nunes TDG, Zhang D, Raissig MT. 2020. Form, development and function of grass stomata. *The Plant Journal* **101**: 780-799.

Obermeier WA, Lehnert LW, Ivanov MA, Luterbacher J, Bendix J. 2018. Reduced summer aboveground productivity in temperate C3 grasslands under future climate regimes. *Earth's Future* **6**: 716-729.

Ogée J, Brunet Y, Loustau D, Berbigier P, Delzon S. 2003. *MuSICA*, a CO_2, water and energy multilayer, multileaf pine forest model: evaluation from hourly to yearly time scales and sensitivity analysis. *Global Change Biology* **9**: 697-717.

Ogée J, Cuntz M, Peylin P, Bariac T. 2007. Non-steady-state, non-uniform transpiration rate and leaf anatomy effects on the progressive stable isotope enrichment of leaf water along monocot leaves. *Plant, Cell & Environment* **30**: 367-387.

Oyewole OA, Inselsbacher E, Näsholm T. 2014. Direct estimation of mass flow and diffusion of nitrogen compounds in solution and soil. *New Phytologist* **201**: 1056-1064.

Pantin F, Simonneau T, Muller B. 2012. Coming of leaf age: control of growth by hydraulics and metabolics during leaf ontogeny. *New Phytologist* **196**: 349-366.

Parrish DJ, Wolf DD. 1983. Kinetics of tall fescue leaf elongation: responses to changes in illumination and vapor pressure. *Crop Science* **23**: 659-663.

Proseus TE, Boyer JS. 2008. Calcium pectate chemistry causes growth to be stored in *Chara corallina*: a test of the pectate cycle. *Plant, Cell & Environment* **31**: 1147-1155.

R Core Team 2020. *R: A language and environment for statistical computing*. Vienna, Austria: R Foundation for Statistical Computing.

Radin JW, Boyer JS. 1982. Control of leaf expansion by nitrogen nutrition in sunflower plants: Role of hydraulic conductivity and turgor. *Plant Physiology* **69**: 771-775.

Reich PB, Hobbie SE, Lee TD. 2014. Plant growth enhancement by elevated CO_2 eliminated by joint water and nitrogen limitation. *Nature Geoscience* **7**: 920-924.

Reich PB, Hungate BA, Luo Y. 2006. Carbon-nitrogen interactions in terrestrial ecosystems in response to rising atmospheric carbon dioxide. *Annual Review of Ecology, Evolution, and Systematics* **37**: 611-636.

Roden J, Siegwolf R. 2012. Is the dual-isotope conceptual model fully operational? *Tree Physiology* **32**: 1179-1182.

Rosbakh S, Auerswald K, Poschlod P. 2021. Rising CO_2 concentrations reduce nitrogen availability in alpine grasslands. *Ecological Indicators* **129**: 107990.

Sardans J, Peñuelas J. 2012. The role of plants in the effects of global change on nutrient availability and stoichiometry in the plant-soil system. *Plant Physiology* **160**: 1741-1761.

Scheidegger Y, Saurer M, Bahn M, Siegwolf R. 2000. Linking stable oxygen and carbon isotopes with stomatal conductance and photosynthetic capacity: a conceptual model. *Oecologia* **125**: 350-357.

Schnyder H, de Visser R. 1999. Fluxes of reserve-derived and currently assimilated carbon and nitrogen in perennial ryegrass recovering from defoliation. The regrowing tiller and its component functionally distinct zones. *Plant Physiology* **119**: 1423-1436.

Schnyder H, Nelson CJ. 1988. Diurnal growth of tall fescue leaf blades. I. Spatial distribution of growth, deposition of water, and assimilate import in the elongation zone. *Plant Physiology* **86**: 1070-1076.

Schnyder H, Schäufele R, Lötscher M, Gebbing T. 2003. Disentangling CO_2 fluxes: direct measurements of mesocosm-scale natural abundance $^{13}CO_2/^{12}CO_2$ gas exchange, ^{13}C discrimination, and labelling of CO_2 exchange flux components in controlled environments. *Plant, Cell & Environment* **26**: 1863-1874.

Schnyder H, Schwertl M, Auerswald K, Schäufele R. 2006. Hair of grazing cattle provides an integrated measure of the effects of site conditions and interannual weather variability on $\delta^{13}C$ of temperate humid grassland. *Global Change Biology* **12**: 1315-1329.

Schnyder H, Seo S, Rademacher IF, Kühbauch W. 1990. Spatial distribution of growth rates and of epidermal cell lengths in the elongation zone during leaf development in *Lolium perenne* L. *Planta* **181**: 423-431.

Seibt U, Rajabi A, Griffiths H, Berry JA. 2008. Carbon isotopes and water use efficiency: sense and sensitivity. *Oecologia* **155**: 441-454.

Seneweera SP, Conroy JP. 2005. Enhanced leaf elongation rates of wheat at elevated CO_2: is it related to carbon and nitrogen dynamics within the growing leaf blade? *Environmental and Experimental Botany* **54**: 174-181.

Serpe MD, Matthews MA. 1994. Changes in cell wall yielding and stored growth in *Begonia argenteo-guttata* L. leaves during the development of water deficits. *Plant and Cell Physiology* **35**: 619-626.

Silvertown J, Poulton P, Johnston E, Edwards G, Heard M, Biss PM. 2006. The Park Grass Experiment 1856–2006: its contribution to ecology. *Journal of Ecology* **94**: 801-814.

Smith NG, Keenan TF. 2020. Mechanisms underlying leaf photosynthetic acclimation to warming and elevated CO_2 as inferred from least-cost optimality theory. *Global Change Biology* **26**: 5202-5216.

Song J, Wan S, Piao S, Knapp AK, Classen AT, Vicca S, Ciais P, Hovenden MJ, Leuzinger S, Beier C, *et al*. 2019. A meta-analysis of 1,119 manipulative experiments on terrestrial carbon-cycling responses to global change. *Nature Ecology & Evolution* **3**: 1309-1320.

Song X, Farquhar GD, Gessler A, Barbour MM. 2014. Turnover time of the non-structural carbohydrate pool influences $\delta^{18}O$ of leaf cellulose. *Plant, Cell & Environment* **37**: 2500-2507.

Sternberg L, Ellsworth PFV. 2011. Divergent biochemical fractionation, not convergent temperature, explains cellulose oxygen isotope enrichment across latitudes. *PLoS ONE* **6**: e28040.

Storkey J, Macdonald AJ, Poulton PR, Scott T, Köhler IH, Schnyder H, Goulding KWT, Crawley MJ. 2015. Grassland biodiversity bounces back from long-term nitrogen addition. *Nature* **528**: 401-404.

Sullivan PF, Welker JM. 2007. Variation in leaf physiology of *Salix arctica* within and across ecosystems in the High Arctic: test of a dual isotope ($\Delta^{13}C$ and $\Delta^{18}O$) conceptual model. *Oecologia* **151**: 372-386.

Tardieu F, Parent B, Simonneau T. 2010. Control of leaf growth by abscisic acid: hydraulic or non-hydraulic processes? *Plant, Cell & Environment* **33**: 636-647.

Tardieu F, Simonneau T, Parent B. 2015. Modelling the coordination of the controls of stomatal aperture, transpiration, leaf growth, and abscisic acid: update and extension of the Tardieu–Davies model. *Journal of Experimental Botany* **66**: 2227-2237.

Terrer C, Jackson RB, Prentice IC, Keenan TF, Kaiser C, Vicca S, Fisher JB, Reich PB, Stocker BD, Hungate BA, *et al*. 2019. Nitrogen and phosphorus constrain the CO_2 fertilization of global plant biomass. *Nature Climate Change* **9**: 684-689.

Terrer C, Vicca S, Hungate BA, Phillips RP, Prentice IC. 2016. Mycorrhizal association as a primary control of the CO_2 fertilization effect. *Science* **353**: 72-74.

Terrer C, Vicca S, Stocker BD, Hungate BA, Phillips RP, Reich PB, Finzi AC, Prentice IC. 2018. Ecosystem responses to elevated CO_2 governed by plant–soil interactions and the cost of nitrogen acquisition. *New Phytologist* **217**: 507-522.

Tholen D, Ethier G, Genty B, Pepin S, Zhu X-G. 2012. Variable mesophyll conductance revisited: theoretical background and experimental implications. *Plant, Cell & Environment* **35**: 2087-2103.

Turner NC. 1981. Techniques and experimental approaches for the measurement of plant water status. *Plant and Soil* **58**: 339-366.

Wang S, Zhang Y, Ju W, Chen JM, Ciais P, Cescatti A, Sardans J, Janssens IA, Wu M, Berry JA, *et al*. 2020. Recent global decline of CO_2 fertilization effects on vegetation photosynthesis. *Science* **370**: 1295-1300.

White AC, Rogers A, Rees M, Osborne CP. 2016. How can we make plants grow faster? A source–sink perspective on growth rate. *Journal of Experimental Botany* **67**: 31-45.

White J, Vaughn B, Michel S 2015. Stable isotopic composition of atmospheric carbon dioxide (^{13}C and ^{18}O) from the NOAA ESRL carbon cycle cooperative global air sampling network, 1990-2014. University of Colorado, Institute of Arctic and Alpine Research (INSTAAR). ftp://aftp.cmdl.noaa.gov/data/trace_gases/co2c13/flask/.

Yu Q, Zhang Y, Liu Y, Shi P. 2004. simulation of the stomatal conductance of winter wheat in response to light, temperature and CO_2 changes. *Annals of Botany* **93**: 435-441.

Acknowledgements

Last, but not least, I would like to thank all the people that contributed to this dissertation, in one way or another.

First of all, I would like to thank my supervisor Prof. Hans Schnyder for all his support throughout my PhD studies. Thank you very much, first, for selecting me for the PhD position and giving me your full trust from the very first day at the Grassland Group until the day when I submitted my dissertation (and beyond). Also, thank you so much for being the best possible supervisor I could have ever imagined. You encouraged and motivated me to be a better scientist and always guided me in the best possible way to overcome all of the academic challenges during this journey. And, finally, I am very grateful for creating such a nice work environment at the institute. I really enjoyed every day that I was there and all of our conversations, be these about my project, science in general or “just” life.

Secondly, I would like to thank my fellow PhD students Regina and Zhu. It was a lot of fun working with you in this project and our exchanges and discussions helped me to improve my research and expand my perspectives. A special thanks also to Rudi, who was always glad to help me with any scientific questions that I could have and gave us the best possible support with all measurements. And to Karl, who has supported me and believed in me since I started at the TUM back in 2014. And, in general, thanks to all colleagues at the Grassland Group. It was really a pleasure working with you all and I wish you the best in the future.

Here, I would also like to thank Dr. Andy Macdonald at Rothamsted Research and Dr. Jérôme Ogée at INRAE for their collaboration with this project.

Finally, thanks to my family and friends who have been by my side in the good and bad moments during this journey. Specially, I thank you, Andrea, my partner for so many years. I would have not been able to do this without you.

5. Appendix A: Publications

The articles included in this thesis, together with the permissions for reproduction, are appended in the following.

Publication 1: Stomatal conductance limited the CO_2 response of grassland in the last century

Juan C Baca Cabrera, Regina T Hirl, Rudi Schäufele, Andy Macdonald, Hans Schnyder

Published in BMC Biology: 19, 50, 2021. doi: 10.1186/s12915-021-00988-4

Publication 2: Atmospheric CO_2 and VPD alter the diel oscillation of leaf elongation in perennial ryegrass: compensation of hydraulic limitation by stored-growth

Juan C Baca Cabrera, Regina T Hirl, Jianjun Zhu, Rudi Schäufele, Hans Schnyder

Published in New Phytologist: 227, 1776–1789, 2020. doi: 10.1111/nph.16639

Publication 3: ^{18}O enrichment of leaf cellulose correlated with ^{18}O enrichment of leaf sucrose but not bulk leaf water in a C_3 grass across contrasts of atmospheric CO_2 concentration and air humidity

Juan C Baca Cabrera, Regina T Hirl, Rudi Schäufele, Jianjun Zhu, Haitao Liu, Jérôme Ogée, Hans Schnyder

Preprint available, doi: 10.21203/rs.3.rs-596094/v1

Publication 4: The ^{18}O ecohydrology of a grassland ecosystem – predictions and observations

Regina T Hirl, Hans Schnyder, Ulrike Ostler, Rudi Schäufele, Inga Schleip, Sylvia H Vetter, Karl Auerswald, Juan C Baca Cabrera, Lisa Wingate, Margaret M Barbour, Jérôme Ogée

Published in Hydrology and Earth System Sciences: 23, 2581–2600, 2019. doi: 10.5194/hess-23-2581-2019

Publication 5: Temperature-sensitive biochemical ^{18}O-fractionation and humidity-dependent attenuation factor are needed to predict $\delta^{18}O$ of cellulose from leaf water in a grassland ecosystem

Regina T Hirl, Jérôme Ogée, Ulrike Ostler, Rudi Schäufele, Juan C Baca Cabrera, Jianjun Zhu, Inga Schleip, Lisa Wingate, Hans Schnyder

Published in New Phytologist: 229, 3156–3171, 2019. doi: 10.1111/nph.17111

6. Appendix B: Lebenslauf